

Natural gradient and parameter estimation for quantum Boltzmann machines

Dhrumil Patel

Department of Computer Science, Cornell University, Ithaca, New York 14850, USA

Mark M. Wilde

School of Electrical and Computer Engineering, Cornell University, Ithaca, New York 14850, USA

(Dated: November 12, 2025)

Thermal states play a fundamental role in various areas of physics, and they are becoming increasingly important in quantum information science, with applications related to semi-definite programming, quantum Boltzmann machine learning, Hamiltonian learning, and the related task of estimating the parameters of a Hamiltonian. Here we establish formulas underlying the basic geometry of parameterized thermal states, and we delineate quantum algorithms for estimating the values of these formulas. More specifically, we establish formulas for the Fisher–Bures and Kubo–Mori information matrices of parameterized thermal states, and our quantum algorithms for estimating their matrix elements involve a combination of classical sampling, Hamiltonian simulation, and the Hadamard test. These results have applications in developing a natural gradient descent algorithm for quantum Boltzmann machine learning, which takes into account the geometry of thermal states, and in establishing fundamental limitations on the ability to estimate the parameters of a Hamiltonian, when given access to thermal-state samples. For the latter task, and for the special case of estimating a single parameter, we sketch an algorithm that realizes a measurement that is asymptotically optimal for the estimation task. We finally stress that the natural gradient descent algorithm developed here can be used for any machine learning problem that employs the quantum Boltzmann machine ansatz.

Keywords: natural gradient, quantum Boltzmann machines, parameterized thermal states, Fisher–Bures information matrix, Kubo–Mori information matrix, Hamiltonian parameter estimation

CONTENTS

I. Introduction	2	B. Natural gradient with respect to the Kubo–Mori metric	8
A. Background	2	C. Example optimization tasks with natural gradient	9
B. Main result	2	VI. Estimation of Hamiltonian parameters from thermal states	9
C. Applications	2	A. Fundamental limitations on multiparameter estimation of thermal states	9
1. Natural gradient descent for quantum Boltzmann machine learning	2	B. Asymptotically optimal strategy for single-parameter estimation of thermal states	9
2. Estimation of Hamiltonian parameters from thermal states	3	VII. Conclusion and future directions	11
D. Paper organization	3	Acknowledgments	11
II. Review of monotone metrics	4	Author contributions	11
A. Fisher–Bures metric	4	References	12
B. Kubo–Mori metric	5		
III. Fisher–Bures and Kubo–Mori information matrices of thermal states	5	A. Additivity of Fisher–Bures information matrix for tensor-product parameterized families	13
IV. Quantum algorithms for estimating the Fisher–Bures and Kubo–Mori information matrices of thermal states	6	B. Proof of Theorem 1	16
A. Quantum Boltzmann–Fisher–Bures estimator	6	C. Proof of Theorem 2	17
B. Quantum Boltzmann–Kubo–Mori estimator	7	D. Review of Hadamard test	19
V. Natural gradient for quantum Boltzmann machine learning	7	E. Estimating the first term of the Fisher–Bures information matrix elements	20
A. Natural gradient with respect to the Fisher–Bures metric	8		

F. Estimating the first term of the Kubo-Mori information matrix elements	23
G. Proof of Theorem 3	24

I. INTRODUCTION

A. Background

Quantum states at thermal equilibrium, known as thermal states, play an essential role in many areas of physics, including condensed matter [1], high energy, and quantum chemistry [2]. They arise from a typical physical process by which a system of interest is weakly coupled to an external environment at a finite temperature [3, Appendix A-1]. Due to their ubiquitous occurrence in nature, they can be used to predict various properties of physical systems. They are also uniquely characterized as being states of maximal entropy subject to an energy constraint [4, 5], the states that minimize the free energy [6, Eqs. (2)–(3)], and completely passive states, whereby no energy can be extracted from them, even when taking multiple copies [7, Section 1.2.2].

In more recent years, thermal states have intersected quantum information science in various intriguing ways. First, quantum algorithms for semidefinite programming make use of them in a fundamental way [8] (see also [9, 10]). As a quantum generalization of classical Boltzmann machines, the model of quantum Boltzmann machines has emerged as a method of performing machine learning tasks on a quantum computer [11–13], with applications to generative modeling [14, 15] and estimating ground-state energies [16]. Finally, there has been interest in performing measurements on thermal states in order to learn the underlying Hamiltonian [17–19] or, related to this goal, to estimate the parameters that uniquely identify a Hamiltonian [20, 21]. All of these applications, in addition to their fundamental role in physics, have motivated the development of quantum algorithms for preparing thermal states [22–29].

B. Main result

In this paper, our fundamental contribution is to establish simple formulas underlying the basic geometry of parameterized thermal states and to construct efficient quantum algorithms for estimating these formulas. We then apply these findings in two different ways: 1) we establish a method for quantum Boltzmann machine learning called natural gradient descent and 2) we prove fundamental limitations on how well one can estimate a Hamiltonian given access to thermal-state samples, in the sense of the Cramer–Rao bound (see (4) and (8) in particular). Here, we consider general parameterized Hamiltonians of

the form

$$G(\theta) := \sum_{j=1}^J \theta_j G_j, \quad (1)$$

where $\theta := (\theta_1, \dots, \theta_J)$ is a parameter vector, $\theta_j \in \mathbb{R}$ and G_j is a fixed Hamiltonian, for all $j \in \{1, \dots, J\}$. Such Hamiltonians lead to thermal states of the following form:

$$\rho(\theta) := \frac{e^{-G(\theta)}}{Z(\theta)}, \quad (2)$$

where the partition function $Z(\theta)$ is defined as

$$Z(\theta) := \text{Tr}[e^{-G(\theta)}]. \quad (3)$$

One of our primary concerns is related to the geometry of such states, as induced by the Fisher–Bures and Kubo–Mori metrics [30], and when doing so, one is naturally led to the notions of the Fisher–Bures and Kubo–Mori information matrices. As some of our main technical contributions, we establish elegant formulas for the elements of the Fisher–Bures and Kubo–Mori information matrices. Of practical relevance, we prove that their matrix elements can be efficiently estimated on a quantum computer, by means of quantum algorithms that we call the *quantum Boltzmann–Fisher–Bures estimator* and the *quantum Boltzmann–Kubo–Mori estimator*, respectively. Let us note here the striking similarity of these algorithms to the recently established quantum Boltzmann gradient estimator [16].

C. Applications

1. Natural gradient descent for quantum Boltzmann machine learning

Our first application is to develop a variant of the standard gradient descent algorithm called natural gradient descent, which specifically applies to quantum Boltzmann machine learning. Importantly, the gradient update step in our approach can be performed efficiently on a quantum computer. We should note that, as in [14, 16], our algorithms for natural gradient descent assume the ability to sample from the thermal state in (2) for every value of the parameter vector θ . So the performance of these algorithms depends on that of thermal-state preparation algorithms [22–29].

Natural gradient was introduced to classical machine learning [31] in order to account for the geometry induced by parameterized probability distributions used in generative modeling. The idea behind the method is that, by incorporating the natural geometry of the problem into the search for a minimum value of the loss function, one can navigate the optimization landscape more judiciously. In contrast, the standard gradient descent algorithm assumes a Euclidean geometry, which is poorly

adapted to the weight space of neural networks due to their intrinsic parameter redundancy [32].

Inspired by the usage of natural gradient for classical machine learning, quantum scientists introduced this method to quantum machine learning implemented with parameterized quantum circuits (PQCs) [33]. This was certainly an interesting theoretical development, and evidence was given that the method works well on particular problem instances. However, there is also evidence that the barren-plateau problem, originally observed for PQCs using standard gradient descent [34–39], persists even when using PQCs supplemented by natural gradient [40]. In contrast, due to the fact that there is evidence that quantum Boltzmann machines do not suffer from the barren-plateau problem in some contexts [14], there is the hope that quantum Boltzmann machine learning supplemented by the natural gradient method developed here will offer a compelling and general approach to machine learning using quantum computers. Let us also note here that natural gradient has been developed for quantum Hamiltonian-based models (distinct from quantum Boltzmann machines), with numerical evidence given regarding its performance for various machine learning tasks [41]. The appendices of [41] also serve as a notable and comprehensive review of the geometry of quantum states.

2. Estimation of Hamiltonian parameters from thermal states

Our second application is to the problem of estimating a Hamiltonian when given access to thermal-state samples. In this context, the following multiparameter Cramer–Rao bound holds for an arbitrary unbiased estimator and for a general parameterized family $(\sigma(\theta))_{\theta \in \mathbb{R}^J}$ of states:

$$\text{Cov}^{(n)}(\hat{\theta}, \theta) \geq \frac{1}{n} [I^{\text{FB}}(\theta)]^{-1}, \quad (4)$$

where $n \in \mathbb{N}$ is the number of copies of the state $\sigma(\theta)$ available, $\hat{\theta}$ is an estimate of the parameter vector θ , the matrix $I^{\text{FB}}(\theta)$ denotes the Fisher–Bures information matrix (defined later in (17)–(18)), and the covariance matrix $\text{Cov}^{(n)}(\hat{\theta}, \theta)$ measures errors in estimation and is defined in terms of its matrix elements as

$$[\text{Cov}^{(n)}(\hat{\theta}, \theta)]_{k, \ell} := \sum_m \text{Tr}[M_m^{(n)} \sigma(\theta)^{\otimes n}](\hat{\theta}_k(m) - \theta_k)(\hat{\theta}_\ell(m) - \theta_\ell). \quad (5)$$

In the above, $(M_m^{(n)})_m$ is an arbitrary positive operator-value measure used for estimation (it satisfies $M_m^{(n)} \geq 0$ for all m and $\sum_m M_m^{(n)} = I^{\otimes n}$). Note that this measurement acts, in general, collectively on all n copies of the state $\sigma(\theta)^{\otimes n}$. Additionally,

$$\hat{\theta}(m) := (\hat{\theta}_1(m), \hat{\theta}_2(m), \dots, \hat{\theta}_J(m)) \quad (6)$$

is a function that maps the measurement outcome m to an estimate $\hat{\theta}(m)$ of the parameter vector θ . See [30, 41–46] for various reviews of quantum Fisher information, geometry of quantum states, and multiparameter estimation.

We stress that (4) is an operator inequality, meaning that it is equivalent to all of the eigenvalues of the operator $\text{Cov}^{(n)}(\hat{\theta}, \theta) - \frac{1}{n} [I^{\text{FB}}(\theta)]^{-1}$ being non-negative. The inequality in (4) was derived for the case $n = 1$ in [47], and the case of general $n \in \mathbb{N}$ follows from the additivity of the Fisher–Bures information matrix with respect to tensor-product states. The latter claim follows from a calculation generalizing that in [48, Appendix D], and we provide it for convenience in Appendix A. Let us finally note that the following operator inequalities hold [30, Eq. (60)]:

$$I^{\text{KM}}(\theta) \geq I^{\text{FB}}(\theta) \geq 0, \quad (7)$$

where $I^{\text{KM}}(\theta)$ denotes the Kubo–Mori information matrix (defined later in (22)–(23)). This inequality implies that $[I^{\text{FB}}(\theta)]^{-1} \geq [I^{\text{KM}}(\theta)]^{-1}$, which in turn implies that $I^{\text{FB}}(\theta)$ gives a better bound on $\text{Cov}^{(n)}(\hat{\theta}, \theta)$ than does $I^{\text{KM}}(\theta)$. As such, we do not consider the matrix $I^{\text{KM}}(\theta)$ in the quantum multiparameter estimation application.

One can formulate a scalar performance metric from (4) by setting W to be a positive semi-definite “weight” matrix and taking the trace of both sides of (4) with respect to W , which leads to

$$\text{Tr}[W \text{Cov}^{(n)}(\hat{\theta}, \theta)] \geq \frac{1}{n} \text{Tr}[W I^{\text{FB}}(\theta)^{-1}]. \quad (8)$$

The left-hand side of (8) should indeed be understood as a performance metric, which weights errors in different ways, so that the inequality in (8) provides a fundamental limitation on the performance of any possible quantum multiparameter estimation scheme. The latter conclusion holds because the right-hand side of (8) has no dependence on the particular scheme being used for estimation and instead only depends on the parameterized family $(\sigma(\theta))_{\theta \in \mathbb{R}^J}$.

The implication of our technical contribution to Hamiltonian parameter estimation is as follows: Our exact formulas for the Fisher–Bures information matrix of the thermal-state family in (2) provide fundamental limitations on the performance of any possible unbiased scheme for estimating the parameter vector θ from performing measurements on the thermal state $\rho(\theta)$. Additionally, for the special case of estimating a single parameter, we sketch an algorithm that realizes a measurement that is asymptotically optimal for the estimation task.

D. Paper organization

In the rest of the paper, we provide more background on the geometry of quantum states induced by the

Fisher–Bures and Kubo–Mori metrics, as well as the related Fisher–Bures and Kubo–Mori information matrices (Section II). After that, we provide our formulas for the elements of the Fisher–Bures and Kubo–Mori information matrices of parameterized thermal states of the form in (2) (Section III), only sketching the idea behind their proofs in the main text while providing detailed proofs in the appendix. We then introduce our quantum algorithms, the quantum Boltzmann–Fisher–Bures and Boltzmann–Kubo–Mori estimators, for estimating the elements of the Fisher–Bures and Kubo–Mori information matrices (Section IV). We finally go into more detail in our two applications: a natural gradient method for quantum Boltzmann machine learning (Section V), and estimating the parameters of a Hamiltonian from copies of a thermal state (Section VI). We conclude in Section VII with a summary and some directions for future work.

II. REVIEW OF MONOTONE METRICS

A. Fisher–Bures metric

When formulating a distance measure between two quantum state vectors $|\psi\rangle$ and $|\phi\rangle$, one might initially guess that the Euclidean distance $\|\psi\rangle - |\phi\rangle\|_2$ would be a reasonable choice. However, in quantum mechanics, this reasoning is misguided because two state vectors $|\psi\rangle$ and $e^{i\varphi}|\psi\rangle$ that differ only by a global phase are physically indistinguishable. In spite of these states being physically indistinguishable, the distance

$$\|\psi\rangle - e^{i\varphi}|\psi\rangle\|_2 = \sqrt{2(1 - \cos(\varphi))} \quad (9)$$

is generally non-zero. As a remedy to this problem, the Bures distance incorporates a minimization over all possible global phases:

$$d_B(\psi, \phi) := \min_{\varphi \in [0, 2\pi]} \|\psi\rangle - e^{i\varphi}|\phi\rangle\|_2 \quad (10)$$

$$= \sqrt{2(1 - |\langle\phi|\psi\rangle|)}, \quad (11)$$

where we have employed the abbreviations $\psi \equiv |\psi\rangle\langle\psi|$ and $\phi \equiv |\phi\rangle\langle\phi|$ and the second equality follows from basic reasoning. The overlap quantity $|\langle\phi|\psi\rangle|$ is known as the root fidelity of the state vectors $|\psi\rangle$ and $|\phi\rangle$.

One can follow the above line of reasoning when generalizing this distance to general states ρ and σ (described by density operators). In doing so, one appeals to the purification principle of quantum mechanics, which states that every density operator ρ_S for a system S can be thought of as the marginal of a pure state ψ_{RS}^ρ of a bipartite system consisting of R and S , so that $\text{Tr}_R[\psi_{RS}^\rho] = \rho_S$. Let ψ_{RS}^σ be a purification of σ_S . It is well known that two states ρ_S and σ_S are equal if and only if there exists a unitary U_R acting on the reference system R such that $|\psi^\rho\rangle_{RS} = (U_R \otimes I_S) |\psi^\sigma\rangle_{RS}$, where $|\psi^\rho\rangle_{RS}$ and $|\psi^\sigma\rangle_{RS}$

are the state vectors corresponding to ψ_{RS}^ρ and ψ_{RS}^σ , respectively. In this way, the unitary U_R generalizes the global phase discussed in the previous paragraph. Furthermore, this line of reasoning then leads to the Bures distance of two general states ρ and σ [49]:

$$d_B(\rho, \sigma) := \min_{U_R} \|\psi^\rho\rangle_{RS} - (U_R \otimes I_S) |\psi^\sigma\rangle_{RS}\|_2 \quad (12)$$

$$= \sqrt{2(1 - \sqrt{F(\rho, \sigma)})}, \quad (13)$$

where the fidelity $F(\rho, \sigma)$ is defined as

$$F(\rho, \sigma) := \|\sqrt{\rho}\sqrt{\sigma}\|_1^2. \quad (14)$$

The equality above is a consequence of Uhlmann's theorem [50], which states that

$$F(\rho, \sigma) = \max_{U_R} |\langle\psi^\sigma|_{RS} (U_R \otimes I_S) |\psi^\rho\rangle_{RS}|^2. \quad (15)$$

The above line of reasoning, as well as its deep connections to quantum estimation theory, underpins why the Bures distance is a natural metric to consider on the space of quantum states.

Now consider a parameterized family $(\sigma(\theta))_{\theta \in \mathbb{R}^J}$ of quantum states, and suppose for simplicity that each state $\sigma(\theta)$ is positive definite (indeed, this is the case for (2), which is the main example that we will consider later on). Then it is well known that the infinitesimal squared line element between two members of the parameterized family is [43, Eq. (77)]

$$d_B^2(\sigma(\theta), \sigma(\theta + d\theta)) = \frac{1}{4} \sum_{i,j=1}^J I_{ij}^{\text{FB}}(\theta) d\theta_i d\theta_j, \quad (16)$$

where $I_{ij}^{\text{FB}}(\theta)$ is a matrix element of a Riemannian metric tensor called the Fisher–Bures information matrix, given explicitly by the following formulas [44, Eqs. (126) and (142)]:

$$I_{ij}^{\text{FB}}(\theta) := \sum_{k,\ell} \frac{2}{\lambda_k + \lambda_\ell} \langle k|\partial_i \sigma(\theta)|\ell\rangle \langle \ell|\partial_j \sigma(\theta)|k\rangle \quad (17)$$

$$= 2 \int_0^\infty ds \text{Tr}[(\partial_i \sigma(\theta)) e^{-s\sigma(\theta)} (\partial_j \sigma(\theta)) e^{-s\sigma(\theta)}]. \quad (18)$$

In the above, we use the shorthand

$$\partial_i \equiv \partial_{\theta_i} \quad (19)$$

and a spectral decomposition $\rho(\theta) = \sum_k \lambda_k |k\rangle\langle k|$, where in the latter notation we have suppressed the dependence of the eigenvalue λ_k and the eigenvector $|k\rangle$ on the parameter vector θ . The second formula in (18) is useful as it is basis independent.

B. Kubo–Mori metric

An alternative metric that one can consider is that induced by the quantum relative entropy, which is defined for states ω and τ as [51]

$$D(\omega\|\tau) := \text{Tr}[\omega(\ln\omega - \ln\tau)] \quad (20)$$

if the support of ω is contained in the support of τ and $D(\omega\|\tau) := +\infty$ otherwise. The quantum relative entropy is a fundamental distinguishability measure in quantum information theory, due to it obeying the data-processing inequality [52] and having an operational meaning in the context of quantum hypothesis testing [53, 54].

Due to the support condition and its related singularity, the metric induced by the quantum relative entropy is not suitable for parameterized families of pure states. However, for our case of interest here, the parameterized thermal states in (2), this is not problematic because all thermal states in (2) are positive definite.

Following reasoning similar to that leading to (16), the infinitesimal line element between two members of the parameterized family $(\sigma(\theta))_{\theta \in \mathbb{R}^J}$ is

$$D(\sigma(\theta)\|\sigma(\theta + d\theta)) = \frac{1}{2} \sum_{i,j=1}^J I_{ij}^{\text{KM}}(\theta) d\theta_i d\theta_j, \quad (21)$$

where $I_{ij}^{\text{KM}}(\theta)$ is a matrix element of a Riemannian metric tensor called the Kubo–Mori information matrix, given explicitly by the following formulas [41, Eqs. (B9), (B12), (B22), (B23)]:

$$\begin{aligned} I_{ij}^{\text{KM}}(\theta) &:= \sum_{k,\ell} c_{\text{KM}}(\lambda_k, \lambda_\ell) \langle k | \partial_i \sigma(\theta) | \ell \rangle \langle \ell | \partial_j \sigma(\theta) | k \rangle \quad (22) \\ &= \int_0^\infty ds \text{Tr}[(\partial_i \sigma)(\sigma + sI)^{-1} (\partial_j \sigma)(\sigma + sI)^{-1}], \quad (23) \end{aligned}$$

where

$$c_{\text{KM}}(x, y) := \begin{cases} \frac{1}{\ln x - \ln y} & \text{if } x = y \\ \frac{\ln x - \ln y}{x - y} & \text{if } x \neq y \end{cases}. \quad (24)$$

In (23), we have used the shorthand $\sigma \equiv \sigma(\theta)$ for brevity. The formula in (23) can be useful, as it is basis independent.

Interestingly, observe that the function $\frac{2}{\lambda_k + \lambda_\ell}$ is the inverse of the arithmetic mean of the eigenvalues λ_k and λ_ℓ , while the function $c_{\text{KM}}(\lambda_k, \lambda_\ell)$ is the inverse of their logarithmic mean.

III. FISHER–BURES AND KUBO–MORI INFORMATION MATRICES OF THERMAL STATES

With this background in place, we move on to state our main technical results (Theorems 1 and 2 below). Before

doing so, let us define Φ_θ to be the following quantum channel:

$$\Phi_\theta(X) := \int_{\mathbb{R}} dt p(t) e^{-iG(\theta)t} X e^{iG(\theta)t}, \quad (25)$$

where

$$p(t) := \frac{2}{\pi} \ln |\coth(\pi t/2)| \quad (26)$$

is a probability density function on $t \in \mathbb{R}$ known as the “high-peak tent” probability density [16], due to its shape when plotted. Prior work [14, 17, 55, 56] refers to the map Φ_θ as the quantum belief propagation superoperator, and it was observed in [16] that it is a quantum channel (a completely positive, trace-preserving map) because $e^{-iG(\theta)t}$ is unitary and, as stated above, $p(t)$ is a probability density function (see also [56, Footnote 32]).

Theorem 1 *For the parameterized family of thermal states in (2), the Fisher–Bures information matrix elements are as follows:*

$$I_{ij}^{\text{FB}}(\theta) = \frac{1}{2} \langle \{\Phi_\theta(G_i), \Phi_\theta(G_j)\} \rangle_{\rho(\theta)} - \langle G_i \rangle_{\rho(\theta)} \langle G_j \rangle_{\rho(\theta)}, \quad (27)$$

where Φ_θ is the quantum channel defined in (25) and $\langle C \rangle_\sigma \equiv \text{Tr}[C\sigma]$.

Let us note the following alternative forms of $I_{ij}^{\text{FB}}(\theta)$ for the family in (2):

$$\begin{aligned} I_{ij}^{\text{FB}}(\theta) &= \text{Re}[\text{Tr}[\Phi_\theta(G_i)\rho(\theta)\Phi_\theta(G_j)]] - \langle G_i \rangle_{\rho(\theta)} \langle G_j \rangle_{\rho(\theta)} \quad (28) \\ &= \frac{1}{2} \text{Tr}[\{\Phi_\theta(G_i) - \mu_i, \Phi_\theta(G_j) - \mu_j\} \rho(\theta)], \quad (29) \end{aligned}$$

where

$$\mu_i := \langle \Phi_\theta(G_i) \rangle_{\rho(\theta)} = \langle G_i \rangle_{\rho(\theta)}. \quad (30)$$

The first expression in (28) is helpful for arriving at the conclusion that each $I_{ij}^{\text{FB}}(\theta)$ can be efficiently estimated on a quantum computer (under the assumption that each G_i is a local operator, acting on a constant number of qubits). The second expression in (29) clarifies that $I^{\text{FB}}(\theta)$ itself is a quantum covariance matrix, implying that $I^{\text{FB}}(\theta) \geq 0$ and as already indicated more generally in (7).

The presence of the quantum channel Φ_θ in (27)–(29) is a hallmark of non-commutativity of the set $\{G_j\}_{j=1}^J$ in (1). If the set $\{G_j\}_{j=1}^J$ is commuting, as is the case for thermal states in classical mechanics, then there is no need for the channel Φ_θ to be present in (27)–(29), and the multiparameter quantum Cramer–Rao bound in (4) is saturated, with the optimal single-copy measurement scheme being to measure each G_i on each copy of $\rho(\theta)$.

The derivation of (27) is rather straightforward when using the following formula for the partial derivative of $\rho(\theta)$:

$$\partial_j \rho(\theta) = -\frac{1}{2} \{\Phi_\theta(G_j), \rho(\theta)\} + \rho(\theta) \langle G_j \rangle_{\rho(\theta)}. \quad (31)$$

This formula is a direct consequence of the developments in [55, Eq. (9)], [57, Proposition 20], and [14, Lemma 5] and its proof was reviewed recently in [16]. Plugging (31) into the expression $\langle k|\partial_i\rho(\theta)|\ell\rangle$ in (17) leads to

$$\langle \ell|\partial_j\rho(\theta)|k\rangle = -\frac{1}{2}\langle \ell|\Phi_\theta(G_j)|k\rangle (\lambda_k + \lambda_\ell) + \delta_{k\ell}\lambda_\ell \langle G_j \rangle_{\rho(\theta)}. \quad (32)$$

Then plugging (32) into (17) and performing some basic algebraic manipulations leads to (27). See Appendix B for details.

We now state our formula for the Kubo–Mori information matrix elements of parameterized thermal states:

Theorem 2 *For the parameterized family of thermal states in (2), the Kubo–Mori information matrix elements are as follows:*

$$I_{ij}^{\text{KM}}(\theta) = \frac{1}{2} \langle \{G_i, \Phi_\theta(G_j)\} \rangle_{\rho(\theta)} - \langle G_i \rangle_{\rho(\theta)} \langle G_j \rangle_{\rho(\theta)}, \quad (33)$$

where Φ_θ is the quantum channel defined in (25) and $\langle C \rangle_\sigma \equiv \text{Tr}[C\sigma]$.

Let us note the following alternative forms of $I_{ij}^{\text{KM}}(\theta)$ for the family in (2):

$$I_{ij}^{\text{KM}}(\theta) = \text{Re}[\text{Tr}[G_i\rho(\theta)\Phi_\theta(G_j)]] - \langle G_i \rangle_{\rho(\theta)} \langle G_j \rangle_{\rho(\theta)} \quad (34)$$

$$= \frac{1}{2} \text{Tr}[\{G_i - \mu_i, \Phi_\theta(G_j) - \mu_j\} \rho(\theta)], \quad (35)$$

where we again made use of (30).

Observe that, interestingly, the only difference between (27) and (33) is the second appearance of the quantum channel Φ_θ in the first term of (27).

The proof of Theorem 2 follows by plugging (32) into (22) and performing a number of algebraic manipulations. See Appendix C for details.

Based on the operator inequality in (7), it follows that

$$v^T I^{\text{KM}}(\theta) v \geq v^T I^{\text{FB}}(\theta) v \quad (36)$$

for every vector $v = (v_1, \dots, v_J)$. Defining $W := \sum_{j=1}^J v_j G_j$, it follows from (36), the expressions in (27) and (33), and the equality $\langle W \rangle_{\rho(\theta)} = \langle \Phi_\theta(W) \rangle_{\rho(\theta)}$ that the following inequality holds:

$$\begin{aligned} \frac{1}{2} \text{Tr}[\{W, \Phi_\theta(W)\} \rho(\theta)] - \left[\langle W \rangle_{\rho(\theta)} \right]^2 \\ \geq \text{Tr}[\Phi_\theta(W)^2 \rho(\theta)] - \left[\langle \Phi_\theta(W) \rangle_{\rho(\theta)} \right]^2. \end{aligned} \quad (37)$$

We note that (37) was proved as [57, Lemma 30]. As such, here we have provided an alternative proof of (37), which is based on the expressions stated in Theorems 1 and 2 and the fundamental inequality in (7), well known in quantum multiparameter estimation.

IV. QUANTUM ALGORITHMS FOR ESTIMATING THE FISHER–BURES AND KUBO–MORI INFORMATION MATRICES OF THERMAL STATES

In this section, we develop our quantum algorithms for estimating the Fisher–Bures and Kubo–Mori information matrix elements given in (27) and (33), respectively. We call them the quantum Boltzmann–Fisher–Bures estimator and the quantum Boltzmann–Kubo–Mori estimator, respectively. Similar to the quantum Boltzmann gradient estimator of [16], they employ a combination of classical random sampling, Hamiltonian simulation [58, 59], and the Hadamard test [60] (the last reviewed in Appendix D).

A. Quantum Boltzmann–Fisher–Bures estimator

We first develop the quantum Boltzmann–Fisher–Bures estimator. Suppose that each G_j in (1) is not only Hermitian but also unitary, as it is for the common case in which each G_j is a tensor product of Pauli operators. Then the second term $\langle G_i \rangle_{\rho(\theta)} \langle G_j \rangle_{\rho(\theta)}$ in (27) can be estimated by means of a quantum algorithm. Since it can be written as

$$\langle G_i \rangle_{\rho(\theta)} \langle G_j \rangle_{\rho(\theta)} = \text{Tr}[(G_i \otimes G_j)(\rho(\theta) \otimes \rho(\theta))], \quad (38)$$

a procedure for estimating it is to generate the state $\rho(\theta) \otimes \rho(\theta)$ and then measure the observable $G_i \otimes G_j$ on these two copies. Through repetition, the estimate of $\langle G_i \rangle_{\rho(\theta)} \langle G_j \rangle_{\rho(\theta)}$ can be made as precise as desired. This procedure is described in detail as [16, Algorithm 2], the result of which is that $O(\varepsilon^{-2} \ln \delta^{-1})$ samples of $\rho(\theta)$ are required to have an accuracy of $\varepsilon > 0$ with a failure probability of $\delta \in (0, 1)$.

We also delineate a quantum algorithm for estimating the first term in (27). It follows by direct substitution of (25), along with further algebraic manipulations, that

$$\begin{aligned} \frac{1}{2} \langle \{\Phi_\theta(G_i), \Phi_\theta(G_j)\} \rangle_{\rho(\theta)} = \\ \int_{\mathbb{R}} \int_{\mathbb{R}} dt_1 dt_2 p(t_1) p(t_2) \text{Re}[\text{Tr}[U_{i,j}(\theta, t_1 - t_2) \rho(\theta)]], \end{aligned} \quad (39)$$

where

$$U_{i,j}(\theta, t) := G_j e^{-iG(\theta)t} G_i e^{iG(\theta)t}. \quad (40)$$

We can then estimate the first term in (27) by a combination of classical random sampling, Hamiltonian simulation [58, 59], and the Hadamard test [60]. This is the key insight behind the quantum Boltzmann–Fisher–Bures estimator. Indeed, the basic idea is to sample t_1 and t_2 independently from the probability density $p(t)$. Based on these choices, we then execute the quantum circuit

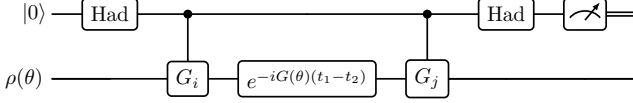


FIG. 1. Quantum circuit that plays a role in realizing an unbiased estimate of $\frac{1}{2} \langle \{\Phi_\theta(G_i), \Phi_\theta(G_j)\} \rangle_{\rho(\theta)}$. The quantum Boltzmann–Fisher–Bures estimator combines this estimate with an unbiased estimate of $\langle G_i \rangle_{\rho(\theta)} \langle G_j \rangle_{\rho(\theta)}$ in order to realize an unbiased estimate of the Fisher–Bures information matrix element $I_{i,j}^{\text{FB}}(\theta)$ in (27).

in Figure 1, which outputs a binary random variable Y , that has a realization $y = 0$ occurring with probability

$$\frac{1}{2} (1 + \text{Re}[\text{Tr}[U_{i,j}(\theta, t_1 - t_2)\rho(\theta)]]) \quad (41)$$

and $y = 1$ occurring with probability

$$\frac{1}{2} (1 - \text{Re}[\text{Tr}[U_{i,j}(\theta, t_1 - t_2)\rho(\theta)]]) . \quad (42)$$

Thus, the expectation of a random variable $Z = (-1)^Y$, conditioned on t_1 and t_2 , is equal to

$$\text{Re}[\text{Tr}[U_{i,j}(\theta, t_1 - t_2)\rho(\theta)]], \quad (43)$$

and including the further averaging over t_1 and t_2 , the expectation is equal to $\text{Tr}[\{\Phi_\theta(G_i), \Phi_\theta(G_j)\} \rho(\theta)]$. As such, we can sample t_1 , t_2 , and Z in this way, and averaging the outcomes gives an unbiased estimate of the first term in (27). This procedure is described in detail in Appendix E as Algorithm 1, the result of which is that $O(\varepsilon^{-2} \ln \delta^{-1})$ samples of $\rho(\theta)$ are required to have an accuracy of $\varepsilon > 0$ with a failure probability of $\delta \in (0, 1)$.

We finally note that this construction can straightforwardly be generalized beyond the case of each G_j being a Pauli string, if they instead are Hermitian operators block encoded into unitary circuits [61, 62].

B. Quantum Boltzmann–Kubo–Mori estimator

Let us now develop the quantum Boltzmann–Kubo–Mori estimator. The second term of (33) is the same as the second term of (27). As such, we can use the same procedure delineated in the paragraph surrounding (38) in order to estimate it.

The first term of (33) is slightly different from the first term of (27), and we can use a similar procedure as outlined in the paragraph surrounding (39) in order to estimate it. We provide details for completeness. It follows by direct substitution of (25), along with further algebraic manipulations, that

$$\frac{1}{2} \text{Tr}[\{G_i, \Phi_\theta(G_j)\} \rho(\theta)] =$$

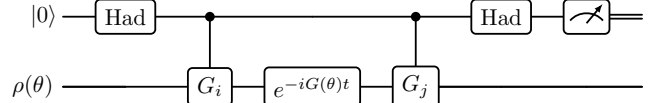


FIG. 2. Quantum circuit that plays a role in realizing an unbiased estimate of $\frac{1}{2} \text{Tr}[\{G_i, \Phi_\theta(G_j)\} \rho(\theta)]$. The quantum Boltzmann–Kubo–Mori estimator combines this estimate with an unbiased estimate of $\langle G_i \rangle_{\rho(\theta)} \langle G_j \rangle_{\rho(\theta)}$ in order to realize an unbiased estimate of the Kubo–Mori information matrix element $I_{i,j}^{\text{KM}}(\theta)$ in (33).

$$\int_{\mathbb{R}} dt p(t) \text{Re}[\text{Tr}[U_{i,j}(\theta, t)\rho(\theta)]], \quad (44)$$

where $U_{i,j}(\theta, t)$ is defined in (40). We can then estimate the first term in (33), as before, by a combination of classical random sampling, Hamiltonian simulation, and the Hadamard test. Indeed, the basic idea is to sample t from the probability density $p(t)$. Based on this choice, we then execute the quantum circuit in Figure 2, which outputs a Rademacher random variable Y , that has a realization $y = +1$ occurring with probability

$$\frac{1}{2} (1 + \text{Re}[\text{Tr}[U_{i,j}(\theta, t)\rho(\theta)]]) \quad (45)$$

and $y = -1$ occurring with probability

$$\frac{1}{2} (1 - \text{Re}[\text{Tr}[U_{i,j}(\theta, t)\rho(\theta)]]) . \quad (46)$$

Thus, the expectation of a random variable $Z = (-1)^Y$, conditioned on t , is equal to

$$\text{Re}[\text{Tr}[U_{i,j}(\theta, t)\rho(\theta)]] \quad (47)$$

and including the further averaging over t , the expectation is equal to $\text{Tr}[\{G_i, \Phi_\theta(G_j)\} \rho(\theta)]$. As such, we can sample t and Z in this way, and averaging the outcomes gives an unbiased estimate of the first term in (33). This procedure is described in detail in Appendix F as Algorithm 2, the result of which is that $O(\varepsilon^{-2} \ln \delta^{-1})$ samples of $\rho(\theta)$ are required to have an accuracy of $\varepsilon > 0$ with a failure probability of $\delta \in (0, 1)$.

V. NATURAL GRADIENT FOR QUANTUM BOLTZMANN MACHINE LEARNING

Our first application of Theorem 1 is to propose a natural gradient descent algorithm for optimizing quantum Boltzmann machines. Before doing so, let us briefly motivate natural gradient descent, following the motivation given in [33]. Let $\mathcal{L}(\theta)$ be a loss function, which is a function of the parameter vector $\theta \in \mathbb{R}^J$. The goal of an optimization algorithm is to minimize the loss $\mathcal{L}(\theta)$,

and the standard gradient descent algorithm does so by means of the following update rule:

$$\theta_{m+1} := \theta_m - \eta \nabla_{\theta} \mathcal{L}(\theta_m), \quad (48)$$

where $\eta > 0$ is the learning rate or step size and $\nabla_{\theta} \mathcal{L}(\theta)$ is the gradient. Given that

$$\theta_m - \eta \nabla_{\theta} \mathcal{L}(\theta_m) = \arg \min_{\theta \in \mathbb{R}^J} \left[\langle \theta - \theta_m, \nabla_{\theta} \mathcal{L}(\theta_m) \rangle + \frac{1}{2\eta} \|\theta - \theta_m\|_2^2 \right], \quad (49)$$

the standard gradient descent algorithm moves in the direction of steepest descent, with respect to ℓ_2 (Euclidean) geometry. As argued previously, this geometry is typically not the correct geometry for the underlying problem and can lead to difficulties when optimizing.

The intuition behind (49) is as follows. We need to choose a point that minimizes the function \mathcal{L} . So, we begin with a linear approximation of this function at the point θ_m :

$$\mathcal{L}(\theta) \approx \mathcal{L}(\theta_m) + \langle \theta - \theta_m, \nabla_{\theta} \mathcal{L}(\theta_m) \rangle. \quad (50)$$

However, directly minimizing the above function leads to a value of $-\infty$ because the above problem is an unconstrained optimization problem. Therefore, we need to add a penalty term to the right-hand side of (50), which forces the optimization to look in the vicinity of the point θ_m :

$$\mathcal{L}(\theta_m) + \langle \theta - \theta_m, \nabla_{\theta} \mathcal{L}(\theta_m) \rangle + \frac{1}{2\eta} \|\theta - \theta_m\|_2^2. \quad (51)$$

In the above, η is the step size which one can tune depending on how much one wants to penalize the objective function. Thus, the resulting constrained optimization problem is to minimize the right-hand side of (51) over all θ , and an optimal choice of θ is given by (49).

A. Natural gradient with respect to the Fisher–Bures metric

For thermal states of the form in (2), the geometry induced by the Fisher–Bures metric is suitable. In order to accommodate it, we modify the optimization problem in (49) to incorporate the Fisher–Bures metric in (16):

$$\theta_{m+1} = \arg \min_{\theta \in \mathbb{R}^J} \left[\langle \theta - \theta_m, \nabla_{\theta} \mathcal{L}(\theta_m) \rangle + \frac{1}{2\eta} \|\theta - \theta_m\|_{g^{\text{FB}}(\theta_m)}^2 \right], \quad (52)$$

where the squared distance measure $\|\theta - \theta_m\|_{g^{\text{FB}}(\theta_m)}^2$ is defined as

$$\|\theta - \theta_m\|_{g^{\text{FB}}(\theta_m)}^2 := \langle \theta - \theta_m, g^{\text{FB}}(\theta_m) (\theta - \theta_m) \rangle, \quad (53)$$

$$[g^{\text{FB}}(\theta)]_{ij} := \frac{1}{4} I_{ij}^{\text{FB}}(\theta). \quad (54)$$

The first-order optimality condition corresponding to (52) is

$$\frac{1}{4} I^{\text{FB}}(\theta_m) (\theta_{m+1} - \theta_m) = -\eta \nabla_{\theta} \mathcal{L}(\theta_m), \quad (55)$$

and solving the above equation for θ_{m+1} gives the following natural gradient descent update rule:

$$\theta_{m+1} = \theta_m - 4\eta [I^{\text{FB}}(\theta_m)]^{-1} \nabla_{\theta} \mathcal{L}(\theta_m), \quad (56)$$

where $[I^{\text{FB}}(\theta)]^{-1}$ is the inverse of the Fisher–Bures information matrix $I^{\text{FB}}(\theta)$ if it is invertible and otherwise it is the pseudoinverse of $I^{\text{FB}}(\theta)$.

Equation (56) gives the basic update rule for any optimization problem that uses the quantum Boltzmann machine ansatz. It delineates a hybrid quantum–classical optimization loop, as is the case with natural gradient for parameterized quantum circuits [33]. Indeed, at each step, one should have a method to evaluate the loss function gradient $\nabla_{\theta} \mathcal{L}(\theta_m)$, and then one can evaluate the J^2 elements of the Fisher–Bures information matrix $I^{\text{FB}}(\theta_m)$, by using the quantum algorithm from Section IV A.

Let us note that the matrix $I^{\text{FB}}(\theta_m)$ is positive definite (and thus invertible) for the common situation in which each G_j acts non-trivially on a constant number of qubits. This follows as a consequence of the last equation of [57, Section 7.2] and the connection made in (37).

B. Natural gradient with respect to the Kubo–Mori metric

An alternative metric to use in natural gradient descent for quantum Boltzmann machines is the Kubo–Mori metric in (21). The reasoning behind the algorithm is the same as given above, and so we highlight only the key differences. Defining

$$\|\theta - \theta_m\|_{g^{\text{KM}}(\theta_m)}^2 := \langle \theta - \theta_m, g^{\text{KM}}(\theta_m) (\theta - \theta_m) \rangle, \quad (57)$$

$$[g^{\text{KM}}(\theta)]_{ij} := \frac{1}{2} I_{ij}^{\text{KM}}(\theta), \quad (58)$$

the basic update rule for natural gradient in terms of the Kubo–Mori metric is as follows:

$$\theta_{m+1} = \theta_m - 2\eta [I^{\text{KM}}(\theta_m)]^{-1} \nabla_{\theta} \mathcal{L}(\theta_m), \quad (59)$$

Due to (7) and the statement at the end of Section V A, it follows that the Kubo–Mori information matrix $I^{\text{KM}}(\theta_m)$ is positive definite (and thus invertible) for the common situation when each G_j acts non-trivially on a constant number of qubits. See also [57, Theorem 28 and Lemma 29] in this context.

C. Example optimization tasks with natural gradient

As a first example, suppose the optimization problem is to estimate the ground-state energy of a Hamiltonian H that is efficiently measurable. One can combine the algorithms from [16] and Section IV to evaluate the update rule in (56). In this case, the loss function is $\mathcal{L}(\theta) = \text{Tr}[H\rho(\theta)]$, and, as shown in [16], each element of the gradient $\nabla_\theta \mathcal{L}(\theta)$ is given by

$$\partial_j \mathcal{L}(\theta) = -\frac{1}{2} \text{Tr}[\{H, \Phi_\theta(G_j)\} \rho(\theta)] + \langle H \rangle_{\rho(\theta)} \langle G_j \rangle_{\rho(\theta)}. \quad (60)$$

One can then use the quantum Boltzmann gradient estimator of [16] to evaluate each element of $\nabla_\theta \mathcal{L}(\theta_m)$, the quantum Boltzmann–Fisher–Bures estimator of Section IV to evaluate each element of $I^{\text{FB}}(\theta_m)$, and then update according to the rule in (56).

Another example lies in generative modeling, using the results of [14]. There, the problem is that a state ω is given, and one desires to generate a state $\rho(\theta)$ that is close to the given state ω . A natural measure of closeness is the quantum relative entropy $D(\omega \parallel \rho(\theta))$, as defined in (20). In this case, we thus set the loss function $\mathcal{L}(\theta) = D(\omega \parallel \rho(\theta))$, and it was shown in [14] that each element of the gradient $\nabla_\theta \mathcal{L}(\theta)$ is given by

$$\partial_j \mathcal{L}(\theta) = \langle H \rangle_{\rho(\theta)} - \langle G_j \rangle_{\rho(\theta)}. \quad (61)$$

Due to this simple form of the gradient, one can use a simple algorithm to evaluate each element of $\nabla_\theta \mathcal{L}(\theta_m)$, the quantum Boltzmann–Fisher–Bures estimator of Section IV to evaluate each element of $I^{\text{FB}}(\theta_m)$, and then update according to the rule in (56).

In both cases, we could alternatively employ natural gradient descent with respect to the Kubo–Mori metric, as given in (59).

These are but two examples of how natural gradient can be used with the quantum Boltzmann machine ansatz, and we note again here that the update rule in (56) can be incorporated into any optimization algorithm that uses the quantum Boltzmann machine ansatz.

Although we do not provide a detailed analysis of the sample complexity of ground-state energy minimization or generative modeling in this paper, as done in the previous works [14, 16], we should note here that, at the least, we expect the number of iterations required for natural gradient to converge to an ε -stationary point to be fewer than those required when performing standard gradient descent. This is due to the advantage that natural gradient has by incorporating the geometry of the landscape when making a decision about which direction navigate to next. We leave it open for now to establish a rigorous convergence analysis for natural gradient with quantum Boltzmann machines.

The main disadvantage of natural gradient descent compared to standard gradient descent is that the update

rules in (56) and (59) require estimating the J^2 parameters in the Fisher–Bures and Kubo–Mori information matrices, respectively. Furthermore, it is necessary to compute their inverses as well. As such, there is a trade-off between this extra sampling and computation time against natural gradient descent’s ability to navigate the landscape more judiciously.

VI. ESTIMATION OF HAMILTONIAN PARAMETERS FROM THERMAL STATES

In this section, we briefly outline our second application, which is to estimating the parameter vector θ , for a Hamiltonian of the form in (1), from thermal states of the form in (2). The setting here is that the tensor-power state $\rho(\theta)^{\otimes n}$, corresponding to n independent copies or samples of $\rho(\theta)$, is available. One then performs a collective measurement $(M_m^{(n)})_m$ on all m copies, followed by classical processing according to the function $\hat{\theta}(m)$ in (6), in order to make an estimate of the parameter vector θ . Under the assumption that the estimator is unbiased, so that

$$\sum_m \text{Tr}[M_m^{(n)} \rho(\theta)^{\otimes n}] \hat{\theta}(m) = \theta, \quad (62)$$

the covariance matrix in (5) is a key figure of merit, determining how well a given estimator performs.

A. Fundamental limitations on multiparameter estimation of thermal states

One of the seminal results in this direction is the multiparameter Cramer–Rao bound of (4). Thus, for our problem at hand, Theorem 1 provides an analytical expression for the Fisher–Bures information matrix of thermal states, and thus in turn limits the performance of any possible estimator. For sufficiently small system sizes, the Fisher–Bures information matrix elements can be calculated analytically. For larger system sizes and for suitable Hamiltonians that meet the assumptions of the quantum Boltzmann–Fisher–Bures estimator, one can estimate the matrix elements by means of this estimator, in order to understand the fundamental limitations on any possible scheme for estimating parameters of Hamiltonians.

B. Asymptotically optimal strategy for single-parameter estimation of thermal states

Our findings also apply to single-parameter estimation, that is, when one is trying to determine a single unknown parameter θ_j from thermal-state samples of the form in (2), and all other parameter values are known. For estimating a single parameter θ_j , an optimal measurement

strategy that saturates the quantum Cramer–Rao bound (corresponding to the j th diagonal entry of (4)) involves measuring in the eigenbasis of the symmetric logarithmic derivative (SLD) operator $L^{(j)}(\theta)$ [63], which is given as follows [44, Eq. (86)]:

$$L^{(j)}(\theta) := \sum_{k,\ell} \frac{2}{\lambda_k + \lambda_\ell} |k\rangle\langle k| \partial_j \rho(\theta) |\ell\rangle\langle \ell|. \quad (63)$$

Note that the SLD satisfies the following differential equation [44, Eq. (83)]:

$$\partial_j \rho(\theta) = \frac{1}{2}(\rho(\theta)L^{(j)}(\theta) + L^{(j)}(\theta)\rho(\theta)). \quad (64)$$

For our case of interest, we have the following result:

Theorem 3 For the parameterized family of thermal states in (2), the SLD operator $L^{(j)}(\theta)$ is given as follows:

$$L^{(j)}(\theta) = -\Phi_\theta(G_j) + \langle G_j \rangle_{\rho(\theta)} I, \quad (65)$$

where Φ_θ is the quantum channel defined in (25) and $\langle C \rangle_\sigma \equiv \text{Tr}[C\sigma]$.

Proof. See Appendix G. ■

See also [21, Appendix C] for an alternative representation of the SLD operator for thermal states. A key distinction between the form in Theorem 3 and that from [21, Appendix C] is that the former leads to a quantum algorithm for measuring in the eigenbasis of the SLD operator $L^{(j)}(\theta)$, as sketched below.

Indeed, Theorem 3 provides an analytical form for the SLD operator, and we know from [63] that the ability to measure in its eigenbasis implies an asymptotically optimal strategy for estimating θ_j , in the sense that it saturates the quantum Cramer–Rao bound. As such, to realize an optimal strategy, we need a method for measuring in the eigenbasis of $\Phi_\theta(G_j)$.

With these notions in place, we now present a sketch of an algorithm that realizes the optimal measurement mentioned above, which involves measuring in the eigenbasis of the SLD operator $L^{(j)}(\theta)$. Having said that, we leave the detailed implementation and rigorous complexity analysis of this algorithm for future work. Our algorithm primarily employs the standard quantum phase estimation (QPE) algorithm to project onto the eigenbasis of the observable $\Phi_\theta(G_j)$. To employ standard QPE, we require controlled Hamiltonian evolutions. For this purpose, we use a Hamiltonian simulation algorithm based on quantum singular value transformation (QSVT) [62]. In this framework, the Hamiltonian of interest, denoted by H , is first block-encoded in a unitary operator [61, 62]. Subsequently, QSVT is employed to implement a polynomial approximation of the target evolution operator e^{-iHt} . In our specific case, the Hamiltonian of interest is $\Phi_\theta(G_j)$.

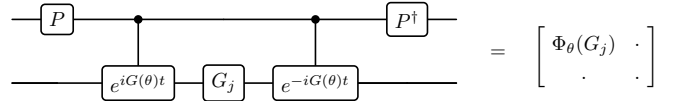


FIG. 3. Block-encoding of the operator $\Phi_\theta(G_j)$.

To begin with, let us discuss how to block-encode $\Phi_\theta(G_j)$. We assume that we have access to a unitary P that prepares the following state:

$$|\varphi(T)\rangle := \sum_{t=0}^{T-1} \sqrt{p_D(t)} |t\rangle, \quad (66)$$

where $p_D(t)$ is a discretization of the probability density in (26), so that $P|0\rangle = |\varphi(T)\rangle$. Note that the discretized probability distribution $p_D(t)$ can realize the channel Φ_θ exactly if a bound on the spectral norm of $G(\theta)$ is available. We also assume that we have access to the inverse unitary P^\dagger . Additionally, we require controlled unitaries $W^{(\pm)}$ defined as controlled Hamiltonian evolutions:

$$W^{(\pm)} := \sum_{t=0}^{T-1} |t\rangle\langle t| \otimes e^{\pm iG(\theta)t}. \quad (67)$$

Then the following unitary block-encodes $\Phi_\theta(G_j)$:

$$(P^\dagger \otimes I) \left(W^{(-)} (I \otimes G_j) W^{(+)} \right) (P \otimes I). \quad (68)$$

The quantum circuit representation of the above unitary is depicted in Figure 3.

That being said, our algorithm for estimating θ_j consists of the following steps:

1. Set $i := 1$.
2. Block-encode $\Phi_\theta(G_j)$ using the aforementioned approach.
3. Prepare the system register in the state $\rho(\theta)$. This state can be written in the eigenbasis $\{|\lambda_r\rangle\}_r$ of $\Phi_\theta(G_j)$ in the following way:
$$\rho(\theta) := \sum_{r,r'} c_{r,r'} |\lambda_r\rangle\langle\lambda_{r'}|. \quad (69)$$
4. Append p control registers and initialize these registers to $|0\rangle^{\otimes p}$.
5. Apply the standard QPE algorithm jointly to the control and system registers, which realizes the following transformation:

$$|0\rangle^{\otimes p}|\lambda_r\rangle \xrightarrow{\text{QPE}} |\tilde{\lambda}_r\rangle|\lambda_r\rangle, \quad (70)$$

where $\tilde{\lambda}_r$ is the closest p -bit estimate of the eigenvalue λ_r , corresponding to the eigenstate $|\lambda_r\rangle$.

6. Measure the control registers in the computational basis and obtain a measurement outcome $\tilde{\lambda}_r$.
7. Set $b_i := \tilde{\lambda}_r$. Set $i := i + 1$.
8. Repeat Steps 2-7 n times.
9. Evaluate $\hat{\theta}_j(b_1, \dots, b_n)$, where $\hat{\theta}_j$ is a classical map that processes the measurement outcomes to produce an estimate of θ_j .

One important caveat to mention, when measuring the observable $\Phi_\theta(G_j)$, is that knowledge of the parameter vector θ is needed to perform the optimal measurement. This kind of problem occurs often in quantum estimation theory [44, Section IV-I], and the typical way around it is to argue that one begins an estimation scheme with a guess of the unknown parameter and adjusts as the estimation scheme proceeds. In our case, this corresponds to making an initial guess for the parameter θ_j , in order to implement the quantum channel Φ_θ , and then as further information is acquired, one adjusts the guess for θ_j and employs the updated guess in future implementations of the channel Φ_θ . We leave the detailed exploration of this kind of strategy for future work, and note here that it is mentioned in [44, Section IV-J] that an iterative scoring algorithm, similar to natural gradient, can be used to iteratively determine an estimate for the unknown parameter θ_j .

VII. CONCLUSION AND FUTURE DIRECTIONS

The main technical results of this paper are exact analytical expressions for the Fisher–Bures and Kubo–Mori information matrix elements of parameterized thermal states (see Theorems 1 and 2). Based on these analytical expressions, we then developed corresponding quantum algorithms, called the quantum Boltzmann–Fisher–Bures and the quantum Boltzmann–Kubo–Mori estimator, which estimate each matrix element of the respective matrix (see Section IV). These results have two applications, in a method for quantum Boltzmann machine learning called natural gradient and in establishing fundamental limitations on our ability to estimate a Hamiltonian from a thermal state of the form in (2). We also sketched an asymptotically optimal approach to single-parameter estimation of thermal states, leaving its detailed study for future work. The natural gradient descent method developed here is general and broad, such that it can be used for any optimization problem that employs the quantum Boltzmann machine ansatz. Combined with the recent findings of [14] and [16], our results here imply that natural gradient descent can be used for both quantum generative modeling and estimating ground-state energies of Hamiltonians, respectively (as outlined at the end of Section V).

In this paper, we have outlined the theory of natural gradient descent with quantum Boltzmann machines,

and in future work, we plan to investigate numerically the performance of the approach. As also mentioned in [16], it remains a pressing open problem to determine whether quantum Boltzmann machine learning suffers from the barren-plateau problem [34–39] that plagues quantum machine learning using parameterized quantum circuits. There is evidence from [14] that quantum Boltzmann machines do not suffer from this problem in certain contexts.

Going forward from here, it is an interesting open problem to determine the sample complexity of natural gradient with quantum Boltzmann machines for problems of interest, such as generative modeling and estimating ground-state energies. Analyses of the performance of natural gradient in the classical case should be helpful for this purpose [64].

Although our statements about limitations on estimation focused on what the Cramer–Rao bound states (see (4) and (8)), one might also wonder what can be said about sample complexity, i.e., the minimum number of copies of $\sigma(\theta)$ that is needed to learn the parameter vector θ with success probability larger than $1 - \delta$ and error less than ε . Here we note that our Fisher information calculations can be combined with a multiparameter generalization of [65, Eq. (53)] to arrive at a sample complexity statement, but we leave a detailed analysis for future work.

Another interesting direction is to explore the connection between mirror descent and natural gradient descent for quantum Boltzmann machines. This connection was recently made in [41], for the case of quantum Hamiltonian-based models and the Kubo–Mori metric. An advantage of mirror descent is that it is a first-order method, as opposed to natural gradient descent, which is a second-order method and furthermore requires an inverse to be calculated. In [41], the two methods were compared for quantum Hamiltonian-based models, and it was found that mirror descent was more robust and stable than natural gradient descent.

ACKNOWLEDGMENTS

DP and MMW acknowledge support from AFRL under agreement no. FA8750-23-2-0031. The U.S. Government is authorized to reproduce and distribute reprints for Governmental purposes notwithstanding any copyright notation thereon. The views and conclusions contained herein are those of the authors and should not be interpreted as necessarily representing the official policies or endorsements, either expressed or implied, of Air Force Research Laboratory or the U.S. Government.

AUTHOR CONTRIBUTIONS

Author Contributions: The following describes the different contributions of the authors of this work, using

roles defined by the CRediT (Contributor Roles Taxonomy) project [66]:

DP: Formal Analysis, Investigation, Methodology, Validation, Writing - Original draft, Writing - Review &

Editing.

MMW: Conceptualization, Formal Analysis, Funding acquisition, Investigation, Methodology, Validation, Writing - Original draft, Writing - Review & Editing.

[1] M. A. Continentino, *Key Methods and Concepts in Condensed Matter Physics*, 2053-2563 (IOP Publishing, 2021).

[2] P. Deglmann, A. Schäfer, and C. Lennartz, Application of quantum calculations in the chemical industry—an overview, *International Journal of Quantum Chemistry* **115**, 107 (2015).

[3] A. M. Alhambra, Quantum many-body systems in thermal equilibrium, *PRX Quantum* **4**, 040201 (2023).

[4] E. T. Jaynes, Information theory and statistical mechanics, *Physical Review* **106**, 620 (1957).

[5] E. T. Jaynes, Information theory and statistical mechanics. II, *Physical Review* **108**, 171 (1957).

[6] G. Giudice, A. Cakan, J. I. Cirac, and M. C. Bañuls, Rényi free energy and variational approximations to thermal states, *Physical Review B* **103**, 205128 (2021).

[7] F. Binder, L. A. Correa, C. Gogolin, J. Anders, and G. Adesso, eds., *Thermodynamics in the quantum regime*, Fundamental Theories of Physics (Springer, 2018).

[8] F. G. S. L. Brandão and K. M. Svore, Quantum speed-ups for solving semidefinite programs, in *2017 IEEE 58th Annual Symposium on Foundations of Computer Science (FOCS)* (IEEE Computer Society, 2017) pp. 415–426.

[9] F. G. S. L. Brandão, A. Kalev, T. Li, C. Y. Lin, K. M. Svore, and X. Wu, Quantum SDP solvers: Large speed-ups, optimality, and applications to quantum learning, in *46th International Colloquium on Automata, Languages, and Programming, ICALP 2019, July 9-12, 2019, Patras, Greece*, LIPIcs, Vol. 132 (Schloss Dagstuhl - Leibniz-Zentrum für Informatik, 2019) pp. 27:1–27:14.

[10] J. van Apeldoorn, A. Gilyén, S. Gribling, and R. de Wolf, Quantum SDP-solvers: Better upper and lower bounds, *Quantum* **4**, 230 (2020).

[11] M. H. Amin, E. Andriyash, J. Rolfe, B. Kulchytskyy, and R. Melko, Quantum Boltzmann machine, *Physical Review X* **8**, 021050 (2018).

[12] M. Benedetti, J. Realpe-Gómez, R. Biswas, and A. Perdomo-Ortiz, Quantum-assisted learning of hardware-embedded probabilistic graphical models, *Physical Review X* **7**, 041052 (2017).

[13] M. Kieferová and N. Wiebe, Tomography and generative training with quantum Boltzmann machines, *Physical Review A* **96**, 062327 (2017).

[14] L. Coopmans and M. Benedetti, On the sample complexity of quantum Boltzmann machine learning, *Communications Physics* **7**, 274 (2024).

[15] C. Tüysüz, M. Demidik, L. Coopmans, E. Rinaldi, V. Croft, Y. Haddad, M. Rosenkranz, and K. Jansen, Learning to generate high-dimensional distributions with low-dimensional quantum Boltzmann machines (2024), arXiv:2410.16363 [quant-ph].

[16] D. Patel, D. Koch, S. Patel, and M. M. Wilde, Quantum Boltzmann machine learning of ground-state energies (2024), arXiv:2410.12935 [quant-ph].

[17] A. Anshu, S. Arunachalam, T. Kuwahara, and M. Soleimanifar, Sample-efficient learning of interacting quantum systems, *Nature Physics* **17**, 931 (2021).

[18] A. Bakshi, A. Liu, A. Moitra, and E. Tang, Learning quantum Hamiltonians at any temperature in polynomial time (2023), arXiv:2310.02243 [quant-ph].

[19] C. Rouzé, D. Stilck Franca, E. Onorati, and J. D. Watson, Efficient learning of ground and thermal states within phases of matter, *Nature Communications* **15**, 7755 (2024).

[20] L. P. García-Pintos, K. Bharti, J. Bringewatt, H. Dehghani, A. Ehrenberg, N. Yunger Halpern, and A. V. Gorshkov, Estimation of Hamiltonian parameters from thermal states, *Physical Review Letters* **133**, 040802 (2024).

[21] P. Abiuso, P. Sekatski, J. Calsamiglia, and M. Perarnau-Llobet, Fundamental limits of metrology at thermal equilibrium (2024), arXiv:2402.06582 [quant-ph].

[22] C.-F. Chen, M. J. Kastoryano, F. G. S. L. Brandão, and A. Gilyén, Quantum thermal state preparation (2023), arXiv:2303.18224 [quant-ph].

[23] C.-F. Chen, M. J. Kastoryano, and A. Gilyén, An efficient and exact noncommutative quantum Gibbs sampler (2023), arXiv:2311.09207 [quant-ph].

[24] T. Bergamaschi, C.-F. Chen, and Y. Liu, Quantum computational advantage with constant-temperature Gibbs sampling (2024), arXiv:2404.14639 [quant-ph].

[25] H. Chen, B. Li, J. Lu, and L. Ying, A randomized method for simulating Lindblad equations and thermal state preparation (2024), arXiv:2407.06594 [quant-ph].

[26] J. Rajakumar and J. D. Watson, Gibbs sampling gives quantum advantage at constant temperatures with $O(1)$ -local Hamiltonians (2024), arXiv:2408.01516 [quant-ph].

[27] C. Rouzé, D. S. Franca, and Á. M. Alhambra, Efficient thermalization and universal quantum computing with quantum Gibbs samplers (2024), arXiv:2403.12691 [quant-ph].

[28] A. Bakshi, A. Liu, A. Moitra, and E. Tang, High-temperature Gibbs states are unentangled and efficiently preivable (2024), arXiv:2403.16850 [quant-ph].

[29] Z. Ding, B. Li, L. Lin, and R. Zhang, Polynomial-time preparation of low-temperature Gibbs states for 2D toric code (2024), arXiv:2410.01206 [quant-ph].

[30] M. Jarzyna and J. Kolodynski, Geometric approach to quantum statistical inference, *IEEE Journal on Selected Areas in Information Theory* **1**, 367 (2020).

[31] S.-I. Amari, Natural gradient works efficiently in learning, *Neural Computation* **10**, 251 (1998).

[32] B. Neyshabur, R. R. Salakhutdinov, and N. Srebro, Path-SGD: Path-normalized optimization in deep neural networks, *Advances in Neural Information Processing Systems* **28** (2015).

[33] J. Stokes, J. Izaac, N. Killoran, and G. Carleo, Quantum natural gradient, *Quantum* **4**, 269 (2020).

[34] J. R. McClean, S. Boixo, V. N. Smelyanskiy, R. Bab

bush, and H. Neven, Barren plateaus in quantum neural network training landscapes, *Nature Communications* **9**, 4812 (2018).

[35] C. O. Marrero, M. Kieferová, and N. Wiebe, Entanglement-induced barren plateaus, *PRX Quantum* **2**, 040316 (2021).

[36] A. Arrasmith, Z. Holmes, M. Cerezo, and P. J. Coles, Equivalence of quantum barren plateaus to cost concentration and narrow gorges, *Quantum Science and Technology* **7**, 045015 (2022).

[37] Z. Holmes, K. Sharma, M. Cerezo, and P. J. Coles, Connecting ansatz expressibility to gradient magnitudes and barren plateaus, *PRX Quantum* **3**, 010313 (2022).

[38] E. Fontana, D. Herman, S. Chakrabarti, N. Kumar, R. Yalovetzky, J. Heredge, S. H. Sureshbabu, and M. Pistotia, Characterizing barren plateaus in quantum ansätze with the adjoint representation, *Nature Communications* **15**, 7171 (2024).

[39] M. Ragone, B. N. Bakalov, F. Sauvage, A. F. Kemper, C. Ortiz Marrero, M. Larocca, and M. Cerezo, A Lie algebraic theory of barren plateaus for deep parameterized quantum circuits, *Nature Communications* **15**, 7172 (2024).

[40] T. Haug, K. Bharti, and M. Kim, Capacity and quantum geometry of parametrized quantum circuits, *PRX Quantum* **2**, 040309 (2021).

[41] F. M. Sbahi, A. J. Martinez, S. Patel, D. Saberi, J. H. Yoo, G. Roeder, and G. Verdon, Provably efficient variational generative modeling of quantum many-body systems via quantum-probabilistic information geometry (2022), arXiv:2206.04663v1 [quant-ph].

[42] I. Bengtsson and K. Zyczkowski, *Geometry of Quantum States: An Introduction to Quantum Entanglement* (Cambridge University Press, 2006).

[43] J. Liu, H. Yuan, X.-M. Lu, and X. Wang, Quantum Fisher information matrix and multiparameter estimation, *Journal of Physics A: Mathematical and Theoretical* **53**, 023001 (2020).

[44] J. S. Sidhu and P. Kok, Geometric perspective on quantum parameter estimation, *AVS Quantum Science* **2**, 014701 (2020).

[45] J. J. Meyer, Fisher information in noisy intermediate-scale quantum applications, *Quantum* **5**, 539 (2021).

[46] M. Scandi, P. Abiuso, J. Surace, and D. D. Santis, Quantum Fisher information and its dynamical nature (2024), arXiv:2304.14984 [quant-ph].

[47] C. Helstrom, The minimum variance of estimates in quantum signal detection, *IEEE Transactions on Information Theory* **14**, 234 (1968).

[48] V. Katariya and M. M. Wilde, Geometric distinguishability measures limit quantum channel estimation and discrimination, *Quantum Information Processing* **20**, 78 (2021).

[49] D. Bures, An extension of Kakutani's theorem on infinite product measures to the tensor product of semifinite W^* -algebras, *Transactions of the American Mathematical Society* **135**, 199 (1969).

[50] A. Uhlmann, The “transition probability” in the state space of a $*$ -algebra, *Reports on Mathematical Physics* **9**, 273 (1976).

[51] H. Umegaki, Conditional expectation in an operator algebra, IV (entropy and information), *Kodai Mathematical Journal* **14**, 59 (1962).

[52] G. Lindblad, Completely positive maps and entropy inequalities, *Communications in Mathematical Physics* **40**, 147 (1975).

[53] F. Hiai and D. Petz, The proper formula for relative entropy and its asymptotics in quantum probability, *Communications in Mathematical Physics* **143**, 99 (1991).

[54] H. Nagaoka and T. Ogawa, Strong converse and Stein's lemma in quantum hypothesis testing, *IEEE Transactions on Information Theory* **46**, 2428 (2000).

[55] M. B. Hastings, Quantum belief propagation: An algorithm for thermal quantum systems, *Physical Review B* **76**, 201102 (2007).

[56] I. H. Kim, Perturbative analysis of topological entanglement entropy from conditional independence, *Physical Review B* **86**, 245116 (2012).

[57] A. Anshu, S. Arunachalam, T. Kuwahara, and M. Soleimanifar, Sample-efficient learning of quantum many-body systems (2020), arXiv:2004.07266v1 [quant-ph].

[58] S. Lloyd, Universal quantum simulators, *Science* **273**, 1073 (1996).

[59] A. M. Childs, D. Maslov, Y. Nam, N. J. Ross, and Y. Su, Toward the first quantum simulation with quantum speedup, *Proceedings of the National Academy of Sciences* **115**, 9456 (2018).

[60] R. Cleve, A. Ekert, C. Macchiavello, and M. Mosca, Quantum algorithms revisited, *Proceedings of the Royal Society A* **454**, 339 (1998).

[61] G. H. Low and I. L. Chuang, Hamiltonian simulation by qubitization, *Quantum* **3**, 163 (2019).

[62] A. Gilyén, Y. Su, G. H. Low, and N. Wiebe, Quantum singular value transformation and beyond: exponential improvements for quantum matrix arithmetics, in *Proceedings of the 51st Annual ACM SIGACT Symposium on Theory of Computing*, STOC 2019 (Association for Computing Machinery, New York, NY, USA, 2019) pp. 193–204.

[63] S. L. Braunstein and C. M. Caves, Statistical distance and the geometry of quantum states, *Physical Review Letters* **72**, 3439 (1994).

[64] G. Desjardins, R. Pascanu, A. Courville, and Y. Bengio, Metric-free natural gradient for joint-training of Boltzmann machines (2013), arXiv:1301.3545 [cs.LG].

[65] J. J. Meyer, S. Khatri, D. Stilck França, J. Eisert, and P. Faist, Quantum metrology in the finite-sample regime, *PRX Quantum* **6**, 030336 (2025).

[66] NISO, Credit – contributor roles taxonomy, <https://credit.niso.org/>, Accessed 2024-10-28.

Appendix A: Additivity of Fisher–Bures information matrix for tensor-product parameterized families

In this appendix, we prove that the Fisher–Bures information matrix is additive with respect to tensor-products. This additivity relation is essential to establishing (4), but it is frequently omitted

in arguments used to establish (4) (see, e.g., the end of [43, Appendix H], where it is simply written “Consider the repetition of experiments (denoted as n), above bound needs to add a factor of $1/n$.”, thus omitting the essential additivity relation). Specifically, we prove the following:

Theorem 4 *Let $(\sigma(\theta))_{\theta \in \mathbb{R}^J}$ and $(\tau(\theta))_{\theta \in \mathbb{R}^J}$ be parameterized families of positive-definite states. Then*

$$I^{\text{FB}}(\theta; (\sigma(\theta) \otimes \tau(\theta))_{\theta \in \mathbb{R}^J}) = I^{\text{FB}}(\theta; (\sigma(\theta))_{\theta \in \mathbb{R}^J}) + I^{\text{FB}}(\theta; (\tau(\theta))_{\theta \in \mathbb{R}^J}). \quad (\text{A1})$$

Proof. Let spectral decompositions of $\sigma(\theta)$ and $\tau(\theta)$ be as follows:

$$\sigma(\theta) = \sum_k \lambda_k(\theta) |\psi_k(\theta)\rangle\langle\psi_k(\theta)|, \quad (\text{A2})$$

$$\tau(\theta) = \sum_m \mu_m(\theta) |\varphi_m(\theta)\rangle\langle\varphi_m(\theta)|. \quad (\text{A3})$$

This implies that

$$\sigma(\theta) \otimes \tau(\theta) = \sum_{k,m} \lambda_k(\theta) \mu_m(\theta) |\psi_k(\theta)\rangle\langle\psi_k(\theta)| \otimes |\varphi_m(\theta)\rangle\langle\varphi_m(\theta)|. \quad (\text{A4})$$

Plugging into (17), we find that

$$\begin{aligned} & I_{ij}^{\text{FB}}(\theta; (\sigma(\theta) \otimes \tau(\theta))_{\theta \in \mathbb{R}^J}) \\ &= 2 \sum_{k,\ell,m,n} \frac{\langle\psi_k(\theta)|\langle\varphi_m(\theta)|\partial_i [\sigma(\theta) \otimes \tau(\theta)]|\psi_\ell(\theta)\rangle|\varphi_n(\theta)\rangle\langle\psi_\ell(\theta)|\langle\varphi_n(\theta)|\partial_j [\sigma(\theta) \otimes \tau(\theta)]|\psi_k(\theta)\rangle|\varphi_m(\theta)\rangle}{\lambda_k(\theta)\mu_m(\theta) + \lambda_\ell(\theta)\mu_n(\theta)}. \end{aligned} \quad (\text{A5})$$

Consider that

$$\partial_i (\sigma(\theta) \otimes \tau(\theta)) = [\partial_i \sigma(\theta)] \otimes \tau(\theta) + \sigma(\theta) \otimes [\partial_i \tau(\theta)]. \quad (\text{A6})$$

This implies that

$$\begin{aligned} & \langle\psi_k(\theta)|\langle\varphi_m(\theta)|\partial_i [\sigma(\theta) \otimes \tau(\theta)]|\psi_\ell(\theta)\rangle|\varphi_n(\theta)\rangle \\ &= \langle\psi_k(\theta)|\langle\varphi_m(\theta)|[[\partial_i \sigma(\theta)] \otimes \tau(\theta) + \sigma(\theta) \otimes [\partial_i \tau(\theta)]]|\psi_\ell(\theta)\rangle|\varphi_n(\theta)\rangle \end{aligned} \quad (\text{A7})$$

$$\begin{aligned} &= \langle\psi_k(\theta)|\langle\varphi_m(\theta)|[[\partial_i \sigma(\theta)] \otimes \tau(\theta)]|\psi_\ell(\theta)\rangle|\varphi_n(\theta)\rangle \\ &\quad + \langle\psi_k(\theta)|\langle\varphi_m(\theta)|[\sigma(\theta) \otimes [\partial_i \tau(\theta)]]|\psi_\ell(\theta)\rangle|\varphi_n(\theta)\rangle \end{aligned} \quad (\text{A8})$$

$$\begin{aligned} &= \langle\psi_k(\theta)|[\partial_i \sigma(\theta)]|\psi_\ell(\theta)\rangle\langle\varphi_m(\theta)|\tau(\theta)|\varphi_n(\theta)\rangle \\ &\quad + \langle\psi_k(\theta)|\sigma(\theta)|\psi_\ell(\theta)\rangle\langle\varphi_m(\theta)|[\partial_i \tau(\theta)]|\varphi_n(\theta)\rangle \end{aligned} \quad (\text{A9})$$

$$= \langle\psi_k(\theta)|[\partial_i \sigma(\theta)]|\psi_\ell(\theta)\rangle\mu_m(\theta)\delta_{mn} + \lambda_k(\theta)\delta_{k\ell}\langle\varphi_m(\theta)|[\partial_i \tau(\theta)]|\varphi_n(\theta)\rangle. \quad (\text{A10})$$

Plugging into (A5), we find that

$$I_{ij}^{\text{FB}}(\theta; (\sigma(\theta) \otimes \tau(\theta))_{\theta \in \mathbb{R}^J}) \quad (\text{A11})$$

$$= 2 \sum_{k,\ell,m,n} \frac{(\langle\psi_k(\theta)|[\partial_i \sigma(\theta)]|\psi_\ell(\theta)\rangle\mu_m(\theta)\delta_{mn} + \lambda_k(\theta)\delta_{k\ell}\langle\varphi_m(\theta)|[\partial_i \tau(\theta)]|\varphi_n(\theta)\rangle)}{\lambda_k(\theta)\mu_m(\theta) + \lambda_\ell(\theta)\mu_n(\theta)} \times$$

$$(\langle\psi_\ell(\theta)|[\partial_j \sigma(\theta)]|\psi_k(\theta)\rangle\mu_m(\theta)\delta_{mn} + \lambda_k(\theta)\delta_{k\ell}\langle\varphi_n(\theta)|[\partial_j \tau(\theta)]|\varphi_m(\theta)\rangle) \quad (\text{A12})$$

$$= 2 \sum_{k,\ell,m,n} \frac{\langle\psi_k(\theta)|[\partial_i \sigma(\theta)]|\psi_\ell(\theta)\rangle\mu_m(\theta)\delta_{mn}\langle\psi_\ell(\theta)|[\partial_j \sigma(\theta)]|\psi_k(\theta)\rangle\mu_m(\theta)\delta_{mn}}{\lambda_k(\theta)\mu_m(\theta) + \lambda_\ell(\theta)\mu_n(\theta)}$$

$$\begin{aligned}
& + 2 \sum_{k,\ell,m,n} \frac{\langle \psi_k(\theta) | [\partial_i \sigma(\theta)] | \psi_\ell(\theta) \rangle \mu_m(\theta) \delta_{mn} \lambda_k(\theta) \delta_{k\ell} \langle \varphi_n(\theta) | [\partial_j \tau(\theta)] | \varphi_m(\theta) \rangle}{\lambda_k(\theta) \mu_m(\theta) + \lambda_\ell(\theta) \mu_n(\theta)} \\
& + 2 \sum_{k,\ell,m,n} \frac{\lambda_k(\theta) \delta_{k\ell} \langle \varphi_m(\theta) | [\partial_i \tau(\theta)] | \varphi_n(\theta) \rangle \langle \psi_\ell(\theta) | [\partial_j \sigma(\theta)] | \psi_k(\theta) \rangle \mu_m(\theta) \delta_{mn}}{\lambda_k(\theta) \mu_m(\theta) + \lambda_\ell(\theta) \mu_n(\theta)} \\
& + 2 \sum_{k,\ell,m,n} \frac{\lambda_k(\theta) \delta_{k\ell} \langle \varphi_m(\theta) | [\partial_i \tau(\theta)] | \varphi_n(\theta) \rangle \lambda_k(\theta) \delta_{k\ell} \langle \varphi_n(\theta) | [\partial_j \tau(\theta)] | \varphi_m(\theta) \rangle}{\lambda_k(\theta) \mu_m(\theta) + \lambda_\ell(\theta) \mu_n(\theta)} \tag{A13}
\end{aligned}$$

$$\begin{aligned}
& = 2 \sum_{k,\ell,m} \frac{\langle \psi_k(\theta) | [\partial_i \sigma(\theta)] | \psi_\ell(\theta) \rangle [\mu_m(\theta)]^2 \langle \psi_\ell(\theta) | [\partial_j \sigma(\theta)] | \psi_k(\theta) \rangle}{[\lambda_k(\theta) + \lambda_\ell(\theta)] \mu_m(\theta)} \\
& + 2 \sum_{k,m} \frac{\langle \psi_k(\theta) | [\partial_i \sigma(\theta)] | \psi_k(\theta) \rangle \mu_m(\theta) \lambda_k(\theta) \langle \varphi_m(\theta) | [\partial_j \tau(\theta)] | \varphi_m(\theta) \rangle}{2 \lambda_k(\theta) \mu_m(\theta)} \\
& + 2 \sum_{k,m} \frac{\lambda_k(\theta) \langle \varphi_m(\theta) | [\partial_i \tau(\theta)] | \varphi_m(\theta) \rangle \langle \psi_k(\theta) | [\partial_j \sigma(\theta)] | \psi_k(\theta) \rangle \mu_m(\theta)}{2 \lambda_k(\theta) \mu_m(\theta)} \\
& + 2 \sum_{k,m,n} \frac{[\lambda_k(\theta)]^2 \langle \varphi_m(\theta) | [\partial_i \tau(\theta)] | \varphi_n(\theta) \rangle \langle \varphi_n(\theta) | [\partial_j \tau(\theta)] | \varphi_m(\theta) \rangle}{\lambda_k(\theta) [\mu_m(\theta) + \mu_n(\theta)]} \tag{A14}
\end{aligned}$$

$$\begin{aligned}
& = 2 \sum_{k,\ell,m} \frac{\langle \psi_k(\theta) | [\partial_i \sigma(\theta)] | \psi_\ell(\theta) \rangle \langle \psi_\ell(\theta) | [\partial_j \sigma(\theta)] | \psi_k(\theta) \rangle}{\lambda_k(\theta) + \lambda_\ell(\theta)} \mu_m(\theta) \\
& + \sum_{k,m} \langle \psi_k(\theta) | [\partial_i \sigma(\theta)] | \psi_k(\theta) \rangle \langle \varphi_m(\theta) | [\partial_j \tau(\theta)] | \varphi_m(\theta) \rangle \\
& + \sum_{k,m} \langle \varphi_m(\theta) | [\partial_i \tau(\theta)] | \varphi_m(\theta) \rangle \langle \psi_k(\theta) | [\partial_j \sigma(\theta)] | \psi_k(\theta) \rangle \\
& + 2 \sum_{k,m,n} \lambda_k(\theta) \frac{\langle \varphi_m(\theta) | [\partial_i \tau(\theta)] | \varphi_n(\theta) \rangle \langle \varphi_n(\theta) | [\partial_j \tau(\theta)] | \varphi_m(\theta) \rangle}{\mu_m(\theta) + \mu_n(\theta)} \tag{A15}
\end{aligned}$$

$$\begin{aligned}
& = 2 \sum_{k,\ell} \frac{\langle \psi_k(\theta) | [\partial_i \sigma(\theta)] | \psi_\ell(\theta) \rangle \langle \psi_\ell(\theta) | [\partial_j \sigma(\theta)] | \psi_k(\theta) \rangle}{\lambda_k(\theta) + \lambda_\ell(\theta)} \\
& + \text{Tr}[\partial_i \sigma(\theta)] \text{Tr}[\partial_j \tau(\theta)] + \text{Tr}[\partial_i \tau(\theta)] \text{Tr}[\partial_j \sigma(\theta)] \\
& + 2 \sum_{m,n} \frac{\langle \varphi_m(\theta) | [\partial_i \tau(\theta)] | \varphi_n(\theta) \rangle \langle \varphi_n(\theta) | [\partial_j \tau(\theta)] | \varphi_m(\theta) \rangle}{\mu_m(\theta) + \mu_n(\theta)} \tag{A16}
\end{aligned}$$

$$= I_{ij}^{\text{FB}}(\theta; (\sigma(\theta))_{\theta \in \mathbb{R}^J}) + I_{ij}^{\text{FB}}(\theta; (\tau(\theta))_{\theta \in \mathbb{R}^J}). \tag{A17}$$

This concludes the proof. ■

Finally, to establish the additivity relation

$$I^{\text{FB}}(\theta; (\sigma^{\otimes n}(\theta))_{\theta \in \mathbb{R}^J}) = n \cdot I^{\text{FB}}(\theta; (\sigma(\theta))_{\theta \in \mathbb{R}^J}), \tag{A18}$$

which we stress again is needed to establish (4), we repeatedly apply (A1) as follows:

$$I^{\text{FB}}(\theta; (\sigma^{\otimes n}(\theta))_{\theta \in \mathbb{R}^J}) = I^{\text{FB}}(\theta; (\sigma(\theta) \otimes \sigma^{\otimes n-1}(\theta))_{\theta \in \mathbb{R}^J}) \tag{A19}$$

$$= I^{\text{FB}}(\theta; (\sigma(\theta))_{\theta \in \mathbb{R}^J}) + I^{\text{FB}}(\theta; (\sigma^{\otimes n-1}(\theta))_{\theta \in \mathbb{R}^J}) \tag{A20}$$

$$= \dots \tag{A21}$$

$$= n \cdot I^{\text{FB}}(\theta; (\sigma(\theta))_{\theta \in \mathbb{R}^J}). \quad (\text{A22})$$

Appendix B: Proof of Theorem 1

Plugging (31) into (17), we find that we should consider the following term:

$$\langle k | \partial_i \rho(\theta) | \ell \rangle = \langle k | \left[-\frac{1}{2} \{ \Phi_\theta(G_i), \rho(\theta) \} + \rho(\theta) \langle G_i \rangle_{\rho(\theta)} \right] | \ell \rangle \quad (\text{B1})$$

$$= -\frac{1}{2} \langle k | \{ \Phi_\theta(G_i), \rho(\theta) \} | \ell \rangle + \langle k | \rho(\theta) | \ell \rangle \langle G_i \rangle_{\rho(\theta)} \quad (\text{B2})$$

$$= -\frac{1}{2} (\langle k | \Phi_\theta(G_i) | \ell \rangle \lambda_\ell + \langle k | \Phi_\theta(G_i) | \ell \rangle \lambda_k) + \delta_{k\ell} \lambda_\ell \langle G_i \rangle_{\rho(\theta)} \quad (\text{B3})$$

$$= -\frac{1}{2} \langle k | \Phi_\theta(G_i) | \ell \rangle (\lambda_k + \lambda_\ell) + \delta_{k\ell} \lambda_\ell \langle G_i \rangle_{\rho(\theta)}. \quad (\text{B4})$$

This implies that

$$\langle \ell | \partial_j \rho(\theta) | k \rangle = -\frac{1}{2} \langle \ell | \Phi_\theta(G_j) | k \rangle (\lambda_k + \lambda_\ell) + \delta_{k\ell} \lambda_\ell \langle G_j \rangle_{\rho(\theta)} \quad (\text{B5})$$

Plugging (B4) and (B5) into (17), we find that

$$\begin{aligned} I_{ij}^{\text{FB}} &= 2 \sum_{k,\ell} \frac{\langle k | \partial_i \rho(\theta) | \ell \rangle \langle \ell | \partial_j \rho(\theta) | k \rangle}{\lambda_k + \lambda_\ell} \\ &= 2 \sum_{k,\ell} \frac{\left[\begin{aligned} &\left(-\frac{1}{2} \langle k | \Phi_\theta(G_i) | \ell \rangle (\lambda_k + \lambda_\ell) + \delta_{k\ell} \lambda_\ell \langle G_i \rangle_{\rho(\theta)} \right) \times \\ &\left(-\frac{1}{2} \langle \ell | \Phi_\theta(G_j) | k \rangle (\lambda_k + \lambda_\ell) + \delta_{k\ell} \lambda_\ell \langle G_j \rangle_{\rho(\theta)} \right) \end{aligned} \right]}{\lambda_k + \lambda_\ell} \quad (\text{B6}) \end{aligned}$$

$$\begin{aligned} &= 2 \sum_{k,\ell} \frac{1}{4} \frac{\langle k | \Phi_\theta(G_i) | \ell \rangle \langle \ell | \Phi_\theta(G_j) | k \rangle (\lambda_k + \lambda_\ell)^2}{\lambda_k + \lambda_\ell} \\ &\quad + 2 \sum_{k,\ell} \left(-\frac{1}{2} \right) \frac{\langle k | \Phi_\theta(G_i) | \ell \rangle (\lambda_k + \lambda_\ell) \delta_{k\ell} \lambda_\ell \langle G_j \rangle_{\rho(\theta)}}{\lambda_k + \lambda_\ell} \\ &\quad + 2 \sum_{k,\ell} \left(-\frac{1}{2} \right) \frac{\langle \ell | \Phi_\theta(G_j) | k \rangle (\lambda_k + \lambda_\ell) \delta_{k\ell} \lambda_\ell \langle G_i \rangle_{\rho(\theta)}}{\lambda_k + \lambda_\ell} \\ &\quad + 2 \sum_{k,\ell} \frac{\delta_{k\ell} \lambda_\ell \langle G_i \rangle_{\rho(\theta)} \delta_{k\ell} \lambda_\ell \langle G_j \rangle_{\rho(\theta)}}{\lambda_k + \lambda_\ell} \quad (\text{B7}) \end{aligned}$$

$$\begin{aligned} &= \frac{1}{2} \sum_{k,\ell} \langle k | \Phi_\theta(G_i) | \ell \rangle \langle \ell | \Phi_\theta(G_j) | k \rangle (\lambda_k + \lambda_\ell) \\ &\quad - \sum_{k,\ell} \langle k | \Phi_\theta(G_i) | \ell \rangle \delta_{k\ell} \lambda_\ell \langle G_j \rangle_{\rho(\theta)} - \sum_{k,\ell} \langle \ell | \Phi_\theta(G_j) | k \rangle \delta_{k\ell} \lambda_\ell \langle G_i \rangle_{\rho(\theta)} \\ &\quad + 2 \sum_{k,\ell} \frac{\delta_{k\ell} \lambda_\ell \langle G_i \rangle_{\rho(\theta)} \delta_{k\ell} \lambda_\ell \langle G_j \rangle_{\rho(\theta)}}{\lambda_k + \lambda_\ell} \quad (\text{B8}) \end{aligned}$$

$$\begin{aligned}
&= \frac{1}{2} \sum_{k,\ell} \langle k | \Phi_\theta(G_i) | \ell \rangle \langle \ell | \Phi_\theta(G_j) | k \rangle \lambda_k + \frac{1}{2} \sum_{k,\ell} \langle k | \Phi_\theta(G_i) | \ell \rangle \langle \ell | \Phi_\theta(G_j) | k \rangle \lambda_\ell \\
&\quad - \sum_k \langle k | \Phi_\theta(G_i) | k \rangle \lambda_k \langle G_j \rangle_{\rho(\theta)} - \sum_k \langle k | \Phi_\theta(G_j) | k \rangle \lambda_k \langle G_i \rangle_{\rho(\theta)} \\
&\quad + 2 \sum_k \frac{\lambda_k^2 \langle G_i \rangle_{\rho(\theta)} \langle G_j \rangle_{\rho(\theta)}}{2\lambda_k}
\end{aligned} \tag{B9}$$

$$\begin{aligned}
&= \frac{1}{2} \text{Tr}[\Phi_\theta(G_j)\rho(\theta)\Phi_\theta(G_i)] + \frac{1}{2} \text{Tr}[\Phi_\theta(G_i)\rho(\theta)\Phi_\theta(G_j)] \\
&\quad - \text{Tr}[\rho(\theta)\Phi_\theta(G_i)] \langle G_j \rangle_{\rho(\theta)} - \text{Tr}[\rho(\theta)\Phi_\theta(G_j)] \langle G_i \rangle_{\rho(\theta)} \\
&\quad + \langle G_i \rangle_{\rho(\theta)} \langle G_j \rangle_{\rho(\theta)}
\end{aligned} \tag{B10}$$

$$\begin{aligned}
&= \frac{1}{2} \text{Tr}[\Phi_\theta(G_j)\rho(\theta)\Phi_\theta(G_i)] + \frac{1}{2} \text{Tr}[\Phi_\theta(G_i)\rho(\theta)\Phi_\theta(G_j)] \\
&\quad - \langle G_i \rangle_{\rho(\theta)} \langle G_j \rangle_{\rho(\theta)}
\end{aligned} \tag{B11}$$

$$= \text{Re}[\text{Tr}[\Phi_\theta(G_j)\rho(\theta)\Phi_\theta(G_i)]] - \langle G_i \rangle_{\rho(\theta)} \langle G_j \rangle_{\rho(\theta)}. \tag{B12}$$

Appendix C: Proof of Theorem 2

Consider that

$$I_{ij}^{\text{KM}} = \sum_{k,\ell} \frac{\ln \lambda_k - \ln \lambda_\ell}{\lambda_k - \lambda_\ell} \langle k | \partial_i \rho(\theta) | \ell \rangle \langle \ell | \partial_j \rho(\theta) | k \rangle \tag{C1}$$

$$= \sum_{k,\ell} \frac{\ln \lambda_k - \ln \lambda_\ell}{\lambda_k - \lambda_\ell} \left[\begin{array}{l} \left(-\frac{1}{2} \langle k | \Phi_\theta(G_i) | \ell \rangle (\lambda_k + \lambda_\ell) + \delta_{k\ell} \lambda_\ell \langle G_i \rangle_{\rho(\theta)} \right) \times \\ \left(-\frac{1}{2} \langle \ell | \Phi_\theta(G_j) | k \rangle (\lambda_k + \lambda_\ell) + \delta_{k\ell} \lambda_\ell \langle G_j \rangle_{\rho(\theta)} \right) \end{array} \right] \tag{C2}$$

$$\begin{aligned}
&= \sum_{k,\ell} \frac{1}{4} \frac{\ln \lambda_k - \ln \lambda_\ell}{\lambda_k - \lambda_\ell} \langle k | \Phi_\theta(G_i) | \ell \rangle \langle \ell | \Phi_\theta(G_j) | k \rangle (\lambda_k + \lambda_\ell)^2 \\
&\quad + \sum_{k,\ell} -\frac{1}{2} \frac{\ln \lambda_k - \ln \lambda_\ell}{\lambda_k - \lambda_\ell} \langle k | \Phi_\theta(G_i) | \ell \rangle (\lambda_k + \lambda_\ell) \delta_{k\ell} \lambda_\ell \langle G_j \rangle_{\rho(\theta)} \\
&\quad + \sum_{k,\ell} -\frac{1}{2} \frac{\ln \lambda_k - \ln \lambda_\ell}{\lambda_k - \lambda_\ell} \langle \ell | \Phi_\theta(G_j) | k \rangle (\lambda_k + \lambda_\ell) \delta_{k\ell} \lambda_\ell \langle G_i \rangle_{\rho(\theta)} \\
&\quad + \sum_{k,\ell} \frac{\ln \lambda_k - \ln \lambda_\ell}{\lambda_k - \lambda_\ell} \delta_{k\ell} \lambda_\ell \langle G_i \rangle_{\rho(\theta)} \delta_{k\ell} \lambda_\ell \langle G_j \rangle_{\rho(\theta)}
\end{aligned} \tag{C3}$$

$$\begin{aligned}
&= \sum_{k,\ell} \frac{1}{4} \frac{(\ln \lambda_k - \ln \lambda_\ell)(\lambda_k + \lambda_\ell)^2}{\lambda_k - \lambda_\ell} \langle k | \Phi_\theta(G_i) | \ell \rangle \langle \ell | \Phi_\theta(G_j) | k \rangle \\
&\quad + \sum_k \left(-\frac{1}{2} \right) \frac{1}{\lambda_k} \langle k | \Phi_\theta(G_i) | k \rangle (2\lambda_k) \lambda_k \langle G_j \rangle_{\rho(\theta)} + \sum_k \left(-\frac{1}{2} \right) \frac{1}{\lambda_k} \langle k | \Phi_\theta(G_j) | k \rangle (2\lambda_k) \lambda_k \langle G_i \rangle_{\rho(\theta)} \\
&\quad + \sum_k \frac{1}{\lambda_k} \lambda_k \langle G_i \rangle_{\rho(\theta)} \lambda_k \langle G_j \rangle_{\rho(\theta)}
\end{aligned} \tag{C4}$$

$$\begin{aligned}
&= \sum_{k,\ell} \frac{1}{4} \frac{(\ln \lambda_k - \ln \lambda_\ell) (\lambda_k + \lambda_\ell)^2}{\lambda_k - \lambda_\ell} \langle k | \Phi_\theta(G_i) | \ell \rangle \langle \ell | \Phi_\theta(G_j) | k \rangle \\
&\quad - \sum_k \langle k | \Phi_\theta(G_i) | k \rangle \lambda_k \langle G_j \rangle_{\rho(\theta)} - \sum_k \langle k | \Phi_\theta(G_j) | k \rangle \lambda_k \langle G_i \rangle_{\rho(\theta)} + \sum_k \langle G_i \rangle_{\rho(\theta)} \lambda_k \langle G_j \rangle_{\rho(\theta)} \quad (\text{C5})
\end{aligned}$$

$$\begin{aligned}
&= \sum_{k,\ell} \frac{1}{4} \frac{(\ln \lambda_k - \ln \lambda_\ell) (\lambda_k + \lambda_\ell)^2}{\lambda_k - \lambda_\ell} \langle k | \Phi_\theta(G_i) | \ell \rangle \langle \ell | \Phi_\theta(G_j) | k \rangle \\
&\quad - \text{Tr} [\rho(\theta) \Phi_\theta(G_i)] \langle G_j \rangle_{\rho(\theta)} - \text{Tr} [\rho(\theta) \Phi_\theta(G_j)] \langle G_i \rangle_{\rho(\theta)} + \langle G_i \rangle_{\rho(\theta)} \langle G_j \rangle_{\rho(\theta)} \quad (\text{C6})
\end{aligned}$$

$$\begin{aligned}
&= \sum_{k,\ell} \frac{1}{4} \frac{(\ln \lambda_k - \ln \lambda_\ell) (\lambda_k + \lambda_\ell)^2}{\lambda_k - \lambda_\ell} \langle k | \Phi_\theta(G_i) | \ell \rangle \langle \ell | \Phi_\theta(G_j) | k \rangle - \langle G_i \rangle_{\rho(\theta)} \langle G_j \rangle_{\rho(\theta)}. \quad (\text{C7})
\end{aligned}$$

The fourth equality is a consequence of the following fact:

$$\lim_{x \rightarrow y} \frac{\ln x - \ln y}{x - y} = \frac{1}{y}. \quad (\text{C8})$$

Now consider that $G(\theta) = \sum_k \mu_k |k\rangle \langle k|$. This implies that for all k , we have $\lambda_k = \frac{e^{-\mu_k}}{Z}$, where Z is the partition function. Plugging this into (C7), we obtain:

$$\begin{aligned}
&\sum_{k,\ell} \frac{1}{4} \frac{(\ln \lambda_k - \ln \lambda_\ell) (\lambda_k + \lambda_\ell)^2}{\lambda_k - \lambda_\ell} \langle k | \Phi_\theta(G_i) | \ell \rangle \langle \ell | \Phi_\theta(G_j) | k \rangle \\
&= \sum_{k,\ell} \frac{1}{4} \frac{\left(\ln \frac{e^{-\mu_k}}{Z} - \ln \frac{e^{-\mu_\ell}}{Z} \right) \left(\frac{e^{-\mu_k}}{Z} + \frac{e^{-\mu_\ell}}{Z} \right)^2}{\frac{e^{-\mu_k}}{Z} - \frac{e^{-\mu_\ell}}{Z}} \langle k | \Phi_\theta(G_i) | \ell \rangle \langle \ell | \Phi_\theta(G_j) | k \rangle \quad (\text{C9})
\end{aligned}$$

$$= \sum_{k,\ell} \frac{1}{4Z} \frac{(-\mu_k + \mu_\ell) (e^{-\mu_k} + e^{-\mu_\ell})^2}{e^{-\mu_k} - e^{-\mu_\ell}} \langle k | \Phi_\theta(G_i) | \ell \rangle \langle \ell | \Phi_\theta(G_j) | k \rangle \quad (\text{C10})$$

$$= \sum_{k,\ell} \frac{1}{4Z} \frac{(-\mu_k + \mu_\ell) (e^{-\mu_k} + e^{-\mu_\ell})}{\frac{e^{-\mu_k} - e^{-\mu_\ell}}{e^{-\mu_k} + e^{-\mu_\ell}}} \langle k | \Phi_\theta(G_i) | \ell \rangle \langle \ell | \Phi_\theta(G_j) | k \rangle \quad (\text{C11})$$

$$= \sum_{k,\ell} \frac{1}{4Z} \frac{(-\mu_k + \mu_\ell) (e^{-\mu_k} + e^{-\mu_\ell})}{\frac{e^{-\mu_k + \mu_\ell - 1}}{e^{-\mu_k + \mu_\ell + 1}}} \langle k | \Phi_\theta(G_i) | \ell \rangle \langle \ell | \Phi_\theta(G_j) | k \rangle \quad (\text{C12})$$

$$= \sum_{k,\ell} \frac{1}{4Z} \frac{(-\mu_k + \mu_\ell) (e^{-\mu_k} + e^{-\mu_\ell})}{\tanh\left(\frac{-\mu_k + \mu_\ell}{2}\right)} \langle k | \Phi_\theta(G_i) | \ell \rangle \langle \ell | \Phi_\theta(G_j) | k \rangle \quad (\text{C13})$$

$$= \sum_{k,\ell} \frac{1}{4Z} \frac{(-\mu_k + \mu_\ell) (e^{-\mu_k} + e^{-\mu_\ell})}{\tanh\left(\frac{-\mu_k + \mu_\ell}{2}\right)} \langle k | \int_{\mathbb{R}} dt p(t) e^{iG(\theta)t} G_i e^{-iG(\theta)t} | \ell \rangle \langle \ell | \Phi_\theta(G_j) | k \rangle \quad (\text{C14})$$

$$\begin{aligned}
&= \sum_{k,\ell} \frac{1}{4Z} \frac{(-\mu_k + \mu_\ell) (e^{-\mu_k} + e^{-\mu_\ell})}{\tanh\left(\frac{-\mu_k + \mu_\ell}{2}\right)} \times \\
&\quad \langle k | \int_{\mathbb{R}} dt p(t) \left(\sum_m |m\rangle \langle m| e^{i\mu_m t} \right) G_i \left(\sum_n |n\rangle \langle n| e^{-i\mu_n t} \right) | \ell \rangle \langle \ell | \Phi_\theta(G_j) | k \rangle \quad (\text{C15})
\end{aligned}$$

$$= \sum_{k,\ell} \frac{1}{4Z} \frac{(-\mu_k + \mu_\ell) (e^{-\mu_k} + e^{-\mu_\ell})}{\tanh\left(\frac{-\mu_k + \mu_\ell}{2}\right)} \int_{\mathbb{R}} dt p(t) e^{i\mu_k t} \langle k | G_i | \ell \rangle e^{-i\mu_\ell t} \langle \ell | \Phi_\theta(G_j) | k \rangle \quad (\text{C16})$$

$$= \sum_{k,\ell} \frac{1}{4Z} \frac{(-\mu_k + \mu_\ell)(e^{-\mu_k} + e^{-\mu_\ell})}{\tanh\left(\frac{-\mu_k + \mu_\ell}{2}\right)} \int_{\mathbb{R}} dt p(t) e^{-i(\mu_\ell - \mu_k)t} \langle k|G_i|\ell\rangle \langle \ell|\Phi_\theta(G_j)|k\rangle \quad (\text{C17})$$

$$= \sum_{k,\ell} \frac{1}{4Z} \frac{(-\mu_k + \mu_\ell)(e^{-\mu_k} + e^{-\mu_\ell})}{\tanh\left(\frac{-\mu_k + \mu_\ell}{2}\right)} \frac{\tanh\left(\frac{-\mu_k + \mu_\ell}{2}\right)}{\frac{(-\mu_k + \mu_\ell)}{2}} \langle k|G_i|\ell\rangle \langle \ell|\Phi_\theta(G_j)|k\rangle \quad (\text{C18})$$

$$= \sum_{k,\ell} \frac{1}{2Z} (e^{-\mu_k} + e^{-\mu_\ell}) \langle k|G_i|\ell\rangle \langle \ell|\Phi_\theta(G_j)|k\rangle \quad (\text{C19})$$

$$= \sum_{k,\ell} \frac{1}{2} \left(\frac{e^{-\mu_k}}{Z} + \frac{e^{-\mu_\ell}}{Z} \right) \langle k|G_i|\ell\rangle \langle \ell|\Phi_\theta(G_j)|k\rangle \quad (\text{C20})$$

$$= \sum_{k,\ell} \frac{1}{2} (\lambda_k + \lambda_\ell) \langle k|G_i|\ell\rangle \langle \ell|\Phi_\theta(G_j)|k\rangle \quad (\text{C21})$$

$$= \frac{1}{2} \text{Tr} [\rho(\theta) G_i \Phi_\theta(G_j)] + \frac{1}{2} \text{Tr} [G_i \rho(\theta) \Phi_\theta(G_j)] \quad (\text{C22})$$

$$= \frac{1}{2} \text{Tr} [\{G_i, \Phi_\theta(G_j)\} \rho(\theta)]. \quad (\text{C23})$$

When combining (C23) with (C7), the proof is concluded.

Appendix D: Review of Hadamard test

In this appendix, we recall a fundamental primitive that estimates the following quantity:

$$\frac{1}{2} \text{Tr} \left[\left(U_1^\dagger U_0 + U_0^\dagger U_1 \right) \rho \right], \quad (\text{D1})$$

where U_0 and U_1 are unitaries and ρ is a quantum state. This primitive was reviewed in [16, Section 6 of Appendix B], and we review it here for convenience. For this primitive, we assume that we have access to multiple copies of ρ . The quantum circuit for this primitive is depicted in Figure 4, where the controlled gate is given by $|0\rangle\langle 0| \otimes U_0 + |1\rangle\langle 1| \otimes U_1$. This circuit consists of the following two quantum registers:

- a control register, initialized in the state $|0\rangle\langle 0|$,
- a system register, which is in the state ρ .

After executing this circuit and obtaining a measurement outcome b in the control register, the final state $\sigma_{\text{sub}}^{(b)}$ (sub-normalized) of the system register is as follows, where $b \in \{0, 1\}$:

$$\sigma_{\text{sub}}^{(b)} = \left(\frac{U_0 + (-1)^b U_1}{2} \right) \rho \left(\frac{U_0^\dagger + (-1)^b U_1^\dagger}{2} \right) \quad (\text{D2})$$

$$= \frac{1}{4} \left(U_0 \rho U_0^\dagger + (-1)^b U_0 \rho U_1^\dagger + (-1)^b U_1 \rho U_0^\dagger + U_1 \rho U_1^\dagger \right). \quad (\text{D3})$$

The probability p_b of obtaining the measurement outcome b is given as:

$$p_b = \text{Tr} \left[\sigma_{\text{sub}}^{(b)} \right] = \frac{2 + (-1)^b \text{Tr} \left[U_0 \rho U_1^\dagger \right] + (-1)^b \text{Tr} \left[U_1 \rho U_0^\dagger \right]}{4} \quad (\text{D4})$$

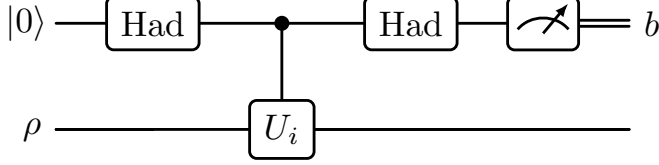


FIG. 4. Quantum primitive for estimating $\frac{1}{2} \text{Tr} \left[(U_1^\dagger U_0 + U_0^\dagger U_1) \rho \right]$.

$$= \frac{2 + (-1)^b \text{Tr} \left[(U_1^\dagger U_0 + U_0^\dagger U_1) \rho \right]}{4}. \quad (\text{D5})$$

Now to estimate the quantity, given by (D1), we employ the following approach. Let b_1, \dots, b_N represent the measurement results obtained from N independent executions of the quantum circuit mentioned above. We define a random variable X as $X := (-1)^b$. The sample mean

$$\bar{X} := \frac{1}{N} \sum_{i=1}^N X_i \quad (\text{D6})$$

serves as an unbiased estimator for the quantity of interest because

$$\mathbb{E}[\bar{X}] = \mathbb{E} \left[\frac{1}{N} \sum_{i=1}^N X_i \right] = \frac{1}{N} \sum_{i=1}^N \mathbb{E}[X_i] = \frac{1}{N} \sum_{i=1}^N \sum_{b_i \in \{0,1\}} p_{b_i} (-1)^{b_i} \quad (\text{D7})$$

$$= \frac{1}{N} \sum_{i=1}^N \left(\frac{2 + \text{Tr} \left[(U_1^\dagger U_0 + U_0^\dagger U_1) \rho \right]}{4} - \frac{2 - \text{Tr} \left[(U_1^\dagger U_0 + U_0^\dagger U_1) \rho \right]}{4} \right) \quad (\text{D8})$$

$$= \frac{1}{2} \text{Tr} \left[(U_1^\dagger U_0 + U_0^\dagger U_1) \rho \right]. \quad (\text{D9})$$

Appendix E: Estimating the first term of the Fisher–Bures information matrix elements

Let us first recall, from the statement of Theorem 1, the expression for the (i, j) -th element of the Fisher–Bures information matrix $I^{\text{FB}}(\theta)$:

$$I_{ij}^{\text{FB}}(\theta) = \frac{1}{2} \text{Tr}[\{\Phi_\theta(G_i), \Phi_\theta(G_j)\} \rho(\theta)] - \langle G_i \rangle_{\rho(\theta)} \langle G_j \rangle_{\rho(\theta)}. \quad (\text{E1})$$

As previously stated in the main text (paragraph surrounding (38)), estimating the second term of the right-hand side of the above equation is straightforward. So, in what follows, we present an algorithm for estimating the first term of the above equation in greater detail.

Consider the following:

$$\begin{aligned} & \frac{1}{2} \text{Tr}[\{\Phi_\theta(G_i), \Phi_\theta(G_j)\} \rho(\theta)] \\ &= \frac{1}{2} (\text{Tr}[\Phi_\theta(G_i) \Phi_\theta(G_j) \rho(\theta)] + \text{Tr}[\Phi_\theta(G_j) \Phi_\theta(G_i) \rho(\theta)]) \\ &= \frac{1}{2} \left(\text{Tr} \left[\int_{\mathbb{R}} \int_{\mathbb{R}} dt_1 dt_2 p(t_1) p(t_2) e^{iG(\theta)t_1} G_i e^{-iG(\theta)t_1} e^{iG(\theta)t_2} G_j e^{-iG(\theta)t_2} \rho(\theta) \right] \right) \end{aligned} \quad (\text{E2})$$

$$+ \text{Tr} \left[\int_{\mathbb{R}} \int_{\mathbb{R}} dt_1 dt_2 p(t_1) p(t_2) e^{iG(\theta)t_2} G_j e^{-iG(\theta)t_2} e^{iG(\theta)t_1} G_i e^{-iG(\theta)t_1} \rho(\theta) \right] \right) \quad (\text{E3})$$

$$= \frac{1}{2} \int_{\mathbb{R}} \int_{\mathbb{R}} dt_1 dt_2 p(t_1) p(t_2) \left(\text{Tr} [e^{iG(\theta)t_1} G_i e^{-iG(\theta)t_1} e^{iG(\theta)t_2} G_j e^{-iG(\theta)t_2} \rho(\theta)] \right. \\ \left. + \text{Tr} [e^{iG(\theta)t_2} G_j e^{-iG(\theta)t_2} e^{iG(\theta)t_1} G_i e^{-iG(\theta)t_1} \rho(\theta)] \right) \quad (\text{E4})$$

$$= \frac{1}{2} \int_{\mathbb{R}} \int_{\mathbb{R}} dt_1 dt_2 p(t_1) p(t_2) \left(\text{Tr} [G_i e^{-iG(\theta)t_1} e^{iG(\theta)t_2} G_j e^{-iG(\theta)t_2} \rho(\theta) e^{iG(\theta)t_1}] \right. \\ \left. + \text{Tr} [e^{iG(\theta)t_2} G_j e^{-iG(\theta)t_2} e^{iG(\theta)t_1} G_i \rho(\theta) e^{-iG(\theta)t_1}] \right) \quad (\text{E5})$$

$$= \frac{1}{2} \int_{\mathbb{R}} \int_{\mathbb{R}} dt_1 dt_2 p(t_1) p(t_2) \left(\text{Tr} [G_i e^{-iG(\theta)t_1} e^{iG(\theta)t_2} G_j e^{-iG(\theta)t_2} e^{iG(\theta)t_1} \rho(\theta)] \right. \\ \left. + \text{Tr} [e^{-iG(\theta)t_1} e^{iG(\theta)t_2} G_j e^{-iG(\theta)t_2} e^{iG(\theta)t_1} G_i \rho(\theta)] \right) \quad (\text{E6})$$

$$= \frac{1}{2} \int_{\mathbb{R}} \int_{\mathbb{R}} dt_1 dt_2 p(t_1) p(t_2) \left(\text{Tr} [G_i e^{-iG(\theta)(t_1-t_2)} G_j e^{iG(\theta)(t_1-t_2)} \rho(\theta)] \right. \\ \left. + \text{Tr} [e^{-iG(\theta)(t_1-t_2)} G_j e^{iG(\theta)(t_1-t_2)} G_i \rho(\theta)] \right) \quad (\text{E7})$$

$$= \int_{\mathbb{R}} \int_{\mathbb{R}} dt_1 dt_2 p(t_1) p(t_2) \left(\frac{1}{2} \text{Tr} \left[\left(G_i e^{-iG(\theta)(t_1-t_2)} G_j e^{iG(\theta)(t_1-t_2)} \right. \right. \right. \\ \left. \left. \left. + e^{-iG(\theta)(t_1-t_2)} G_j e^{iG(\theta)(t_1-t_2)} G_i \right) \rho(\theta) \right] \right). \quad (\text{E8})$$

We are now in a position to present an algorithm (Algorithm 1) to estimate the first term of (E1) using its equivalent form mentioned above. At the core of our algorithm lies a quantum primitive (refer to Appendix D for more details) that estimates a quantity of the form given by

$$\frac{1}{2} \text{Tr} \left[\left(U_1^\dagger U_0 + U_0^\dagger U_1 \right) \rho \right]. \quad (\text{E9})$$

Note that by substituting $U_1 = G_i e^{-iG(\theta)(t_1-t_2)} G_j$, $U_0 = e^{-iG(\theta)(t_1-t_2)}$, and $\rho = \rho(\theta)$ into the equation above, we recover the expression inside the integral of (E8). To this end, the quantum circuit of the primitive with these values of U_0 and U_1 is depicted in Figure 1.

Algorithm 1 estimate_first_term_FB($i, j, \theta, \{G_\ell\}_{\ell=1}^J, \varepsilon, \delta$)

1: **Input:** Indices $i, j \in [J]$, parameter vector $\theta = (\theta_1, \dots, \theta_J)^\top \in \mathbb{R}^J$, Gibbs local Hamiltonians $\{G_\ell\}_{\ell=1}^J$, precision $\varepsilon > 0$, error probability $\delta \in (0, 1)$
2: $N \leftarrow \lceil 2 \ln(2/\delta)/\varepsilon^2 \rceil$
3: **for** $n = 0$ to $N - 1$ **do**
4: Initialize the control register to $|0\rangle\langle 0|$
5: Prepare the system register in the state $\rho(\theta)$
6: Sample t_1 and t_2 independently at random with probability $p(t)$ (defined in (26))
7: Apply the Hadamard gate to the control register
8: Apply the following unitaries to the control and system registers:
9: • Controlled- G_i : G_i is a local unitary with the control on the control register
10: • $e^{-iG(\theta)(t_1-t_2)}$: Hamiltonian simulation for time $t_1 - t_2$ on the system register
11: • Controlled- G_j : G_j is a local unitary with the control on the control register
12: Apply the Hadamard gate to the control register
13: Measure the control register in the computational basis and store the measurement outcome b_n
14: $Y_n^{(\text{FB})} \leftarrow (-1)^{b_n}$
15: **end for**
16: **return** $\bar{Y}^{(\text{FB})} \leftarrow \frac{1}{N} \sum_{n=0}^{N-1} Y_n^{(\text{FB})}$

We now show that the output of Algorithm 1, i.e., $\bar{Y}^{(\text{FB})}$, is an unbiased estimator of the first term of (E1):

$$\mathbb{E}[\bar{Y}^{(\text{FB})}] = \mathbb{E}\left[\frac{1}{N} \sum_{n=0}^{N-1} Y_n^{(\text{FB})}\right] = \mathbb{E}\left[\frac{1}{N} \sum_{n=0}^{N-1} (-1)^{b_n}\right] \quad (\text{E10})$$

$$= \frac{1}{N} \sum_{n=0}^{N-1} \mathbb{E}[(-1)^{b_n}] = \frac{1}{N} \sum_{n=0}^{N-1} \sum_{b_n \in \{0,1\}} p_{b_n} [(-1)^{b_n}]. \quad (\text{E11})$$

Observe that

$$p_{b_n} := \int_{\mathbb{R}} \int_{\mathbb{R}} dt_1 dt_2 p(t_1)p(t_2) \left(\frac{2 + (-1)^{b_n} \text{Tr}[(U_1^\dagger U_0 + U_0^\dagger U_1) \rho(\theta)]}{4} \right). \quad (\text{E12})$$

This is because in Algorithm 1, we first sample t_1 and t_2 independently at random with probability $p(t)$ and then apply the primitive introduced in Appendix D with $U_1 = G_i e^{-iG(\theta)(t_1-t_2)} G_j$, $U_0 = e^{-iG(\theta)(t_1-t_2)}$, whose probability of outputting a bit b is given by (D5). Substituting the above expression for p_{b_n} into (E11), we get

$$\begin{aligned} & \mathbb{E}[\bar{Y}^{(\text{FB})}] \\ &= \frac{1}{N} \sum_{n=0}^{N-1} \sum_{b_n \in \{0,1\}} \left(\int_{\mathbb{R}} \int_{\mathbb{R}} dt_1 dt_2 p(t_1)p(t_2) \left(\frac{2 + (-1)^{b_n} \text{Tr}[(U_1^\dagger U_0 + U_0^\dagger U_1) \rho(\theta)]}{4} \right) \right) [(-1)^{b_n}] \end{aligned} \quad (\text{E13})$$

$$= \int_{\mathbb{R}} \int_{\mathbb{R}} dt_1 dt_2 p(t_1)p(t_2) \left(\frac{1}{N} \sum_{n=0}^{N-1} \sum_{b_n \in \{0,1\}} \left(\frac{2 + (-1)^{b_n} \text{Tr}[(U_1^\dagger U_0 + U_0^\dagger U_1) \rho(\theta)]}{4} \right) [(-1)^{b_n}] \right) \quad (\text{E14})$$

$$= \int_{\mathbb{R}} \int_{\mathbb{R}} dt_1 dt_2 p(t_1)p(t_2) \left(\frac{1}{2} \text{Tr}[(U_1^\dagger U_0 + U_0^\dagger U_1) \rho(\theta)] \right) \quad (\text{E15})$$

$$\begin{aligned}
&= \int_{\mathbb{R}} \int_{\mathbb{R}} dt_1 dt_2 p(t_1) p(t_2) \left(\frac{1}{2} \text{Tr} \left[\left(G_i e^{-iG(\theta)(t_1-t_2)} G_j e^{iG(\theta)(t_1-t_2)} \right. \right. \right. \\
&\quad \left. \left. \left. + e^{-iG(\theta)(t_1-t_2)} G_j e^{iG(\theta)(t_1-t_2)} G_i \right) \rho(\theta) \right] \right), \tag{E16}
\end{aligned}$$

where the third equality follows directly from (D9).

Appendix F: Estimating the first term of the Kubo-Mori information matrix elements

To begin, we recall from the statement of Theorem 2 the expression for the (i, j) -th element of the Kubo-Mori information matrix:

$$I_{ij}^{\text{KM}}(\theta) = \frac{1}{2} \langle \{G_i, \Phi_{\theta}(G_j)\} \rangle_{\rho(\theta)} - \langle G_i \rangle_{\rho(\theta)} \langle G_j \rangle_{\rho(\theta)}, \tag{F1}$$

Here, as well, the estimation of the second term of the above equation is relatively straightforward. Therefore, in what follows, we focus on estimating the first term. Consider the following:

$$\frac{1}{2} \langle \{G_i, \Phi_{\theta}(G_j)\} \rangle_{\rho(\theta)} = \frac{1}{2} \int_{\mathbb{R}} dt p(t) \text{Tr} \left[\{G_i, e^{-iG(\theta)t} G_j e^{iG(\theta)t}\} \rho(\theta) \right] \tag{F2}$$

$$= \frac{1}{2} \int_{\mathbb{R}} dt p(t) \text{Tr} \left[(G_i e^{-iG(\theta)t} G_j e^{iG(\theta)t} + e^{-iG(\theta)t} G_j e^{iG(\theta)t} G_i) \rho(\theta) \right] \tag{F3}$$

In a similar vein to our previous approach for estimating the first term of the Fisher-Bures information matrix elements, we employ the primitive presented in Appendix D here as well. This time, we set $U_1 = G_i e^{-iG(\theta)t} G_j$ and $U_0 = e^{-iG(\theta)t}$, and the quantum circuit of the primitive with these values of U_0 and U_1 is depicted in Figure 2. To this end, we present an algorithm (Algorithm 2) for estimating $\frac{1}{2} \langle \{G_i, \Phi_{\theta}(G_j)\} \rangle_{\rho(\theta)}$. This algorithm outputs an unbiased estimator $\bar{Y}^{(\text{KM})}$ of the quantity of interest, and the proof of this unbiasedness follows similarly to the analysis of Algorithm 1 shown in Appendix E.

Algorithm 2 estimate_first_term_KM($i, j, \theta, \{G_{\ell}\}_{\ell=1}^J, \varepsilon, \delta$)

- 1: **Input:** Indices $i, j \in [J]$, parameter vector $\theta = (\theta_1, \dots, \theta_J)^T \in \mathbb{R}^J$, Gibbs local Hamiltonians $\{G_{\ell}\}_{\ell=1}^J$, precision $\varepsilon > 0$, error probability $\delta \in (0, 1)$
- 2: $N \leftarrow \lceil 2 \ln(2/\delta) / \varepsilon^2 \rceil$
- 3: **for** $n = 0$ to $N - 1$ **do**
- 4: Initialize the control register to $|0\rangle\langle 0|$
- 5: Prepare the system register in the state $\rho(\theta)$
- 6: Sample t with probability $p(t)$ (defined in (26))
- 7: Apply the Hadamard gate to the control register
- 8: Apply the following unitaries to the control and system registers:
 - Controlled- G_i : G_i is a local unitary with the control on the control register
 - $e^{-iG(\theta)t}$: Hamiltonian simulation for time t on the system register
 - Controlled- G_j : G_j is a local unitary with the control on the control register
- 9: Apply the Hadamard gate to the control register
- 10: Measure the control register in the computational basis and store the measurement outcome b_n
- 11: $Y_n^{(\text{KM})} \leftarrow (-1)^{b_n}$
- 12: **end for**
- 13: **return** $\bar{Y}^{(\text{KM})} \leftarrow \frac{1}{N} \sum_{n=0}^{N-1} Y_n^{(\text{KM})}$

Appendix G: Proof of Theorem 3

Recall that the (k, ℓ) -th element of the SLD operator $L^{(j)}(\theta)$ is given as follows:

$$L_{k\ell}^{(j)}(\theta) = \frac{2\langle k|\partial_j\rho(\theta)|\ell\rangle}{\lambda_k + \lambda_\ell}. \quad (\text{G1})$$

Plugging (B5) into the above equation, we find that

$$L_{k\ell}^{(j)}(\theta) = \frac{2\left(-\frac{1}{2}\langle k|\Phi_\theta(G_j)|\ell\rangle(\lambda_k + \lambda_\ell) + \delta_{k,\ell}\lambda_\ell\langle G_j\rangle_{\rho(\theta)}\right)}{\lambda_k + \lambda_\ell} \quad (\text{G2})$$

$$= \frac{-\langle k|\Phi_\theta(G_j)|\ell\rangle(\lambda_k + \lambda_\ell)}{\lambda_k + \lambda_\ell} + \frac{2\delta_{k,\ell}\lambda_\ell\langle G_j\rangle_{\rho(\theta)}}{\lambda_k + \lambda_\ell} \quad (\text{G3})$$

$$= -\langle k|\Phi_\theta(G_j)|\ell\rangle + \frac{2\lambda_k\langle G_j\rangle_{\rho(\theta)}}{2\lambda_k}\delta_{k,\ell} \quad (\text{G4})$$

$$= -\langle k|\Phi_\theta(G_j)|\ell\rangle + \langle G_j\rangle_{\rho(\theta)}\delta_{k,\ell}. \quad (\text{G5})$$

This implies that

$$L^{(j)}(\theta) = \sum_{k,\ell} L_{k\ell}^{(j)}(\theta)|k\rangle\langle\ell| \quad (\text{G6})$$

$$= \sum_{k,\ell} \left(-\langle k|\Phi_\theta(G_j)|\ell\rangle + \langle G_j\rangle_{\rho(\theta)}\delta_{k,\ell}\right)|k\rangle\langle\ell| \quad (\text{G7})$$

$$= -\Phi_\theta(G_j) + \langle G_j\rangle_{\rho(\theta)}I. \quad (\text{G8})$$